

**Revised version (Clean copy)****TITLE:**

**Redundancy and Complementarity between ERAP1 and ERAP2 Revealed by their Effects on the Behçet's Disease-Associated HLA-B\*51 Peptidome.**

**Authors:**

Pablo Guasp<sup>1</sup>, Elena Lorente<sup>1</sup>, Adrian Martín-Esteban<sup>1</sup>, Eilon Barnea<sup>2</sup>, Paolo Romania<sup>3</sup>,  
Doriana Fruci<sup>3</sup>, Jonas J. W. Kuiper<sup>4</sup>, Arie Admon<sup>2</sup> and José A. López de Castro<sup>1</sup>.

**Affiliation:**

<sup>1</sup>Centro de Biología Molecular Severo Ochoa (CSIC-UAM), 28049 Madrid, Spain; <sup>2</sup>Faculty of Biology, Technion - Israel Institute of Technology, Haifa 32000, Israel; <sup>3</sup>Immuno-Oncology Laboratory, Paediatric Haematology/Oncology Department, Ospedale Pediatrico Bambino Gesù, IRCCS, Rome, Italy; <sup>4</sup>Department of Ophthalmology, Laboratory of Translational Immunology, University Medical Center, Utrecht University, Utrecht, The Netherlands.

**Running Title:**

ERAP1 and ERAP2 interplay in the HLA-B\*51 peptidome

*Address correspondence to:* Dr. José A. López de Castro. Centro de Biología Molecular Severo Ochoa, c/Nicolás Cabrera, N. 1, Universidad Autónoma, 28049 Madrid, Spain. Phone: 34-91 196 4554. Email: aldecastro@cbm.csic.es

## Abstract

The endoplasmic reticulum aminopeptidases ERAP1 and ERAP2 trim peptides to be loaded onto HLA molecules, including the main risk factor for Behçet's disease HLA-B\*51. ERAP1 is also a risk factor among HLA-B\*51-positive individuals, whereas no association is known with ERAP2. This study addressed the mutual relationships between both enzymes in the processing of an HLA-bound peptidome, interrogating their differential association with Behçet's disease. CRISPR/Cas9 was used to generate knock outs of ERAP1, ERAP2 or both from transfectant 721.221-HLA-B\*51:01 cells. The surface expression of HLA-B\*51 was reduced in all cases. The effects of depleting each or both enzymes on the B\*51:01 peptidome were analyzed by quantitative label-free mass spectrometry. Substantial quantitative alterations of peptide length, subpeptidome balance, N-terminal residue usage, affinity and presentation of non-canonical ligands were observed. These effects were often different in the presence or absence of the other enzyme, revealing their mutual dependency. In the absence of ERAP1, ERAP2 showed similar and significant processing of B\*51:01 ligands, indicating functional redundancy. The high overlap between the peptidomes of wildtype and double KO cells indicates that a large majority of B\*51:01 ligands are present in the ER even in the absence of ERAP1/ERAP2. These results indicate that both enzymes have distinct, but complementary and partially redundant effects on the B\*51:01 peptidome, leading to its optimization and maximal surface expression. The distinct effects of both enzymes on the HLA-B\*51 peptidome provide a basis for their differential association with Behçet's disease and suggest a pathogenetic role of the B\*51:01 peptidome.

**Word count:** 248

## INTRODUCTION

Major Histocompatibility Complex Class I (MHC-I) molecules present peptides on the surface of every nucleated cell to be recognized by the T-cell receptors (TCR) of CD8<sup>+</sup> T-cells and the Killer-cell immunoglobulin-like receptors (KIR) of Natural Killer (NK) cells (1-4). MHC-I ligands arise mainly from intracellular proteins and defective ribosomal products (5) that are degraded in the cytosol by the proteasome and other proteases. A small fraction of the resulting products (6) enter the endoplasmic reticulum (ER) through the transporter associated with antigen processing (TAP) (7). ERAP1 and ERAP2, both members of the oxytocinase subfamily of M1 Zn-metallopeptidases (8), trim the N-terminal peptide residues to the correct length for loading onto the MHC-I molecules, which are then exported to the cell surface (9,10). These enzymes can also destroy MHC-I ligands by over-trimming (11).

ERAP1 is expressed in all individuals and is encoded by a highly polymorphic gene whose allelic variants are complex allotypes, usually referred to as haplotypes (Hap), which include multiple non-synonymous single nucleotide polymorphisms (SNPs), with significant impact on the enzymatic activity of the protein (12-18). The most common ERAP1 variants, accounting for about 99% of those found in human populations, are termed Hap1 to Hap10 (19).

ERAP1 preferentially cleaves N-terminal hydrophobic residues, shows a poor performance with basic and acidic ones, and does not cleave peptide bonds involving Pro (20). Due to a mechanism known as “molecular ruler”, which is seemingly unique to ERAP1, this enzyme is strongly affected by substrate length, efficiently trimming peptides from 10-16 amino acid residues, being less efficient for 9-mers and virtually inactive with 8-mers and shorter peptides (11,21).

Although ERAP2 shares about 50% sequence identity with ERAP1 (22), it shows significant differences in expression, polymorphism and enzymatic properties (23,24). There is only one common ERAP2 SNP (rs2549782, leading to the K392N amino acid change) known to alter the enzymatic activity (25). However, due to linkage disequilibrium with another SNP (rs2248374) that induces nonsense-mediated decay of the RNA transcript, this variant is rare in the general population (26). Thus, about 25% of individuals, those homozygous for the G allele

of rs2248374, are ERAP2-negative, and most of those who are ERAP2-positive express only the K392 variant. In addition, ERAP2 shows preference for N-terminal basic residues (10,22), although it can trim a few others (23). Like ERAP1 and most other aminopeptidases (27), ERAP2 is unable to trim peptide bonds involving Pro. Unlike ERAP1, it does not follow the “molecular ruler” mechanism, and is less efficient in trimming 10-mers and longer peptides than shorter ones (28).

A unique family of inflammatory diseases are strongly associated with particular MHC-I alleles. The most prominent of these associations concern birdshot chorioretinopathy, ankylosing spondylitis, psoriasis and Behçet’s disease with HLA-A\*29:02 (29,30), HLA-B\*27 (31,32), HLA-C\*06:02 (33,34) and HLA-B\*51 (35-37), respectively. ERAP1 and/or ERAP2 are susceptibility factors for all of these diseases, but show distinct patterns of genetic association (38). Thus, ERAP1 is associated with birdshot chorioretinopathy (39), ankylosing spondylitis (13), psoriasis (40), and Behçet’s disease (41) in individuals carrying the corresponding MHC-I susceptibility alleles. The risk and protective ERAP1 haplotypes are disease-dependent. For instance, the low activity Hap10 haplotype is protective for ankylosing spondylitis and psoriasis (19), but is a risk factor for birdshot chorioretinopathy (39) and Behçet’s disease (42). ERAP2 is associated with birdshot chorioretinopathy, ankylosing spondylitis and psoriasis, although not in epistasis with the MHC-I susceptibility allele in the two latter diseases (43-46). The epistatic nature of its association with birdshot chorioretinopathy (29,39) cannot be statistically interrogated because virtually all patients are A\*29:02 positive (30). ERAP2 expression is the risk factor in all cases. This enzyme is not associated, to the best of our knowledge, with Behçet’s disease.

The association of ERAP1 and ERAP2 with these diseases and the alterations induced by both enzymes on the disease-associated MHC-I peptidomes (38), together with the absence of a common risk haplotype in ERAP1, strongly suggest a pathogenetic role of peptides.

The present study specifically addressed the distinct contribution of ERAP1 and ERAP2 on shaping the peptidome of the Behçet’s disease-associated HLA-B\*51:01 molecule. Behçet’s disease is a multisystemic autoinflammatory disorder characterized by genital ulceration, oral

aphthae, uveitis, skin lesions and joint inflammation (47). The etiology of the disease is unknown, but multiple immunological components are involved, including autoreactive HLA-B\*51-restricted CD8<sup>+</sup> T cells (48) and NK cells (49-51).

Several features of the HLA-B\*51 peptidome are particularly suitable for distinguishing the role of ERAP1 and ERAP2 in antigen processing, for assessing the influence of ERAP2 on ERAP1 trimming suggested by *in vitro* studies (52,53) and for addressing the issue that ERAP2 is not a risk factor for Behçet's disease. These features are: the subpeptidome structure, a relatively high frequency of 8-mers, and a very low frequency of N-terminal (P1) basic residues among HLA-B\*51 ligands (54-56).

HLA-B\*51 binds mainly peptides with Ala or Pro at peptide position 2 (P2), and Ile, Val or Leu at the C-terminal position (PC). The peptides with Pro2 show globally higher affinity for HLA-B\*51 than those with Ala2 and very different patterns of P1 residue usage (55). Since X-Pro bonds are cleaved by neither ERAP1 nor ERAP2, only the Ala2 subpeptidome can be modified by over-trimming. Thus, the different processing features of the two subpeptidomes allow us to define the role of ERAP1 and ERAP2 on peptide subsets whose generation/destruction balance can be affected in distinct ways by each of these enzymes. Moreover, since ERAP1 and ERAP2 have different substrate length preferences they can contribute in distinct ways to shaping the length of the peptidomes, an effect that can be particularly well assessed on MHC-I molecules binding a significant percentage of 8-mers, such as HLA-B\*51.

ERAP2 is known to reduce the amounts of peptides with basic P1 residues in the HLA-B\*27 and HLA-A\*29:02 peptidomes (57-59). Since the frequency of such peptides is quite low among HLA-B\*51 ligands (55), a direct effect of ERAP2 on destruction of HLA-B\*51 ligands might be much smaller. Thus, the possible activation of ERAP1 trimming by ERAP2 may be particularly well assessed on the HLA-B\*51 peptidome. In addition, the possible relationship between the low preference of HLA-B\*51 for peptides with basic P1 residues and the apparent lack of association of ERAP2 with Behçet's disease can be approached from these studies.

To assess the role of ERAP1 and ERAP2, both in the presence and in the absence of each other, on the HLA-B\*51 peptidome, we generated ERAP1 KO, ERAP2 KO and double ERAP1/ERAP2 KO/KO lines from the transfectant lymphoblastoid cell line (LCL) 721.221-B\*51:01 and compared their respective peptidomes. This approach allowed us, for the first time to our knowledge, to separately establish the contribution of each enzyme, and their mutual influence, to shaping an MHC-I peptidome in live cells.

## EXPERIMENTAL PROCEDURES

*Cell lines and generation of ERAP1 and ERAP2 KO by CRISPR.* The human LCL 721.221 does not express HLA-A,B,C molecules on the cell surface (60). This cell line is both ERAP1 and ERAP2 positive and is heterozygous for the Behçet's disease protective Hap1 and Hap8 haplotypes of ERAP1 (55,61). RMA-S is a TAP-deficient murine cell line (H-2<sup>b</sup>) derived from the T-cell lymphoma RBL-5 (62). The transfectant cell lines 721.221-B\*51:01 (55,61) and RMA-S-B\*51:01 (63) were kindly provided by Prof. Masafumi Takiguchi (Center for AIDS Research, Kumamoto University, Kumamoto, Japan) and were used for immunopeptidomics and binding studies, respectively.

ERAP1 and ERAP2 KO cell lines were derived from 721.221-B\*51:01. For the generation of ERAP1 KO cell lines the Alt-R CRISPR-Cas9 system (Integrated DNA Technologies, Coralville, Iowa, US) was used as indicated by the manufacturer and cells were electroporated with the Neon Transfection System (Thermo Fisher Scientific, Waltham, Massachusetts, US). Briefly, the crRNA GCTATCGGAAGAACCCTGC was pre-incubated with the Alt-R tracrRNA at 95°C for 5 min, cooled down at room temperature and mixed with the Alt-R S.p. Cas9 Nuclease. After incubating for 10 min, about  $8 \times 10^5$  721.221-B\*51:01 cells were mixed with the crRNA: tracrRNA-Cas9 mix and electroporated with two pulses of 1100 V and 30 ms each. Electroporated cells were immediately taken up in antibiotic-free medium for 3 days and single clones were isolated by limiting dilution. Two ERAP1 KO clonal populations were isolated, designated as 3.35 and 3.36. The same protocol was used with the crRNA CTAATGGGGAACGATTCCT on the 721.221-B\*51:01 and 3.35 cells for the generation of

the ERAP2 KO and ERAP1/2 KO/KO cell lines, respectively. The procedures used induced a double-strand break in exon 2 of the ERAP1 and ERAP2 genes, within codon 120 and between codons 62 and 63, respectively.

The following cell clones were expanded for immuno-peptidomics analyses: the ERAP1 KO clone 3.36 (E1KO), one ERAP2 KO clone (E2KO), and two ERAP1/2 double KO/KO (E1E2KO) clones, designated as E1E2KO #1 and E1E2KO #19, respectively. The polyclonal transfectant cell line 721.221-B\*51:01 was considered as the wild type (WT). All cell lines were grown in RPMI 1640 medium supplemented with 25mM HEPES buffer, 2mM L-glutamine, 5% Fetal Bovine Serum (FBS) (Gibco, Thermo Fisher Scientific), penicillin and streptomycin, and, in the case of RMA-S-B\*51:01, 0.15mg/ml Hygromycin B.

*Generation of ERAP1KO with shRNA.* To account for possible off-target effects affecting the B\*51:01 peptidome, an independently generated 721.221-B\*51:01 transfectant cell line was used and ERAP1 was knocked down with shRNA. For the generation of ERAP1 shRNA cell line, 721.221-B\*5101 cells were transduced with lentiviral particles containing shRNA vectors. Briefly, lentiviral particles were generated in HEK293T cells by combining a pLKO.1 plasmid containing shRNA sequences, packaging plasmid pCMV-dR8.74, and envelope plasmid VSV-G/pMD2.G. 721.221-B\*5101 cells were infected by the spin inoculation method with lentivirus containing a non-target shRNA control vector (SHC002) or the ERAP1 shRNA (TRCN0000060542) (Sigma-Aldrich) and transduced cells were selected with 2 µg/ml puromycin for 3 days.

*Western Blotting and Flow cytometry.* The expression of ERAP1, ERAP2 and γ-tubulin proteins was assessed by Western Blot as previously described (64) using the monoclonal antibodies (mAb) 6H9, 3F5 (both from R&D Systems, Minneapolis, Minnesota, US) and GTU88 (Sigma-Aldrich, San Luis, Missouri, US), respectively.

Flow cytometry was performed as previously described (65) with minor modifications. Briefly, cells were cultured in fresh medium at a starting concentration of  $1 \times 10^5$  cells/ml. After 48h incubation,  $1 \times 10^5$  cells per point were collected, washed and stained in FACS Buffer (PBS, 2% bovine serum albumin, 0.5mM EDTA) using 50 µl of the mAb W6/32 (IgG2a, specific for a monomorphic HLA-I determinant) (66) at 20 µg/ml or HC-10 (IgG2a, specific for free HLA-I heavy chains) (67) at 50 µg/ml. Cells were washed and stained with the secondary antibody

Goat anti-Mouse IgG (H+L) FITC conjugate (Thermo Fisher Scientific) and fluorescence was analyzed in a FACSCalibur Flow Cytometer (BD Biosciences, San Diego, USA).

*Isolation of HLA-B\*51-bound Peptides and Mass Spectrometry.* HLA-B\*51-bound peptides were isolated from  $1 \times 10^9$  cells per individual preparation exactly as previously described (55). Three independent preparations were used from each cell line to provide biological replicates. Samples were analyzed in a Q-Exactive-Plus mass spectrometer (Thermo Fisher Scientific) as previously described (68). The peptides were resolved with a 7-40% acetonitrile gradient with 0.1% formic acid for 180 min and 0.15  $\mu$ L/min on a capillary column pressure-packed with Reprosil C18-Aqua (Dr. Maisch, GmbH, Ammerbuch-Entringen, Germany) as in (69). The dynamic exclusion was set to 20 sec. The selected masses were fragmented from the survey scan of the mass-to-charge ratio ( $m/z$ ) 300-1,800 AMU at a resolution of 70,000. MS/MS spectra were acquired starting at  $m/z$  200 with a resolution of 17,500. The target value was set to  $1 \times 10^5$  and the isolation window to 1.8  $m/z$ . Peptide sequences were assigned from the MS/MS spectra as detailed in the paragraph on Experimental Design and Strategy (see Below).

*Epitope Stabilization Assay.* The experimental binding affinity of two HLA-B\*51 natural ligands and their P1 and P2 modified analogs was measured with an epitope stabilization assay using RMA-S-B\*51:01 cells as previously described (70). Peptide DAYETTLHV was identified as an HLA-B\*51 ligand in the present study; peptide LPPVVAKEI is an HIV-derived epitope that was previously crystallized in complex with HLA-B\*51 (71). The following P1 and P2 modified versions of these ligands were also used: LAYETTLHV, LPYETTLHV, DPYETTLHV, DPPVVAKEI, DAPVVAKEI and LAPVVAKEI. Synthetic peptides with a purity >90.7% were purchased from BIO BASIC (Markham, ON, Canada).

RMA-S-B\*51:01 cells were cultured at 26°C for 16-24 h, then incubated at  $2 \times 10^5$  cells/well for 3h at 26°C in the presence of various peptide concentrations in a final volume of 100  $\mu$ l PBS with 20% FBS, and again for 3h at 37°C in the same conditions. The HLA-B\*27 ligand KRLEEIMKR was used as negative control. MHC-I/peptide complex stabilization was measured by flow cytometry using the mAb TP25.99SF (IgG1, anti HLA-A+B+C  $\alpha$ 3 specific, EXBIO, Vestec, Czech Republic) as described above. The EC50 value for each peptide was



calculated as the concentration yielding 50% of the maximum stabilization reached with a strong B\*51:01 binder, LPSDFFPSV (72,73), used as positive control.

*Theoretical binding affinity.* The theoretical binding affinity of HLA-B\*51:01 ligands was calculated using the NetMHCcons 1.1 Server (<http://www.cbs.dtu.dk/services/NetMHCcons/>) as described (74)

*Statistical analyses.* Differences in residue frequencies were analyzed using the  $\chi^2$  test with Bonferroni's correction when applicable. Relative intensity differences among peptide sets were assessed by an unpaired t-test. Differences in the theoretical affinity of peptides were assessed by the Mann-Whitney test. In all cases  $p < 0.05$  was considered as statistically significant.

*Experimental Design and Strategy.* The purpose of this study was to determine the contribution of ERAP1, ERAP2 and the combination of both enzymes to shaping the HLA-B\*51:01 peptidome in live cells. To this end ERAP1 KO, ERAP2 KO and ERAP1+2 KO clonal lines, hereafter designated as E1KO, E2KO, and E1E2KO, respectively, were generated by CRISPR from 721.221-B\*51:01 transfectant cells. The effects of depleting one or both enzymes on the HLA-B\*51 peptidome were analyzed by quantitative label-free MS. The analysis addressed the three following questions: 1) the effects of ERAP1 depletion in either the presence or absence of ERAP2, which were examined by comparing the B\*51:01 peptidomes from WT vs E1KO ( $E1^+E2^+/E1^-E2^+$ ) and E2KO vs E1E2KO ( $E1^+E2^-/E1^-E2^-$ ), 2) the effects of ERAP2 depletion in either the presence or absence of ERAP1, which were examined in the WT vs E2KO ( $E1^+E2^+/E1^+E2^-$ ) and E1KO vs E1E2KO ( $E1^-E2^+/E1^-E2^-$ ) comparisons, 3) the effects of the joint absence of ERAP1 and ERAP2, which were examined in the WT vs E1E2KO ( $E1^+E2^+/E1^-E2^-$ ) comparison. Three independent preparations of the HLA-B\*51:01-bound peptides were obtained from each cell line to provide biological replicates (**Figure S1**) and enable label-free quantitative comparisons of B\*51:01 ligands.

The peptide pools from each individual preparation were separately subjected to MS and the peptides were assigned from the MS/MS spectra using the MaxQuant software (version 1.5.8.3) (75) with the Andromeda search engine (76) and the human UniProt/Swiss-Prot database (release 20-4-17: 70946 entries) under the following parameters: precursor ion mass

and fragment mass tolerance 20 ppm, false discovery rate (FDR) 0.01 and peptide-spectrum matching (PSM) FDR 0.05, oxidation (Met), acetylation (protein N-terminus) and Gln to Pyro-Glu conversion were included as variable modifications. No fixed modifications were included. Identifications derived from the reverse database and known contaminants were eliminated.

The canonical HLA-B\*51 ligands were selected from the total peptide assignments based on the following criteria: 1) peptides 8 to 12 residues long, corresponding to the large majority of MHC-I ligands, and 2) peptides carrying the previously defined HLA-B\*51:01 motif of Pro or Ala at P2 and Ile, Leu or Val at PC (55). Peptides fulfilling both criteria include the vast majority of the HLA-B\*51 peptidome and were used for most subsequent analyses. Peptides having only the P2 or the PC motif of HLA-B\*51, including N-terminal and C-terminal extensions of canonical sequences, were considered as non-canonical B\*51 ligands and were analyzed separately.

The global differences among the peptidomes from the various cell lines were assessed by comparing the length, P2 and PC usage from the total canonical peptides, as well as the percentages of non-canonical ones, from each cell line.

Quantitative differences in peptide amounts between cell lines were assigned in pairwise comparisons as follows. In each experiment the intensity of any given ion peak was normalized to the total intensity of the canonical HLA-B\*51 ligands shared between the two cell lines compared. The mean normalized intensity of each ion peak from the three individual experiments for each cell line was taken as the amount of that peptide in that cell line relative to the total amount of canonical ligands shared between the cell lines compared. The HLA-B\*51 ligands in each pairwise comparison were classified on the basis of the normalized intensity ratio (IR) of the corresponding ion peak in the two cell lines. Peptides predominant in one cell line, relative to the other, that is with  $IR > 1.0$ , were subdivided in two subsets: peptides with  $IR > 1.0$  to 1.5 (hereafter abbreviated as  $IR > 1.0-1.5$ ) in either cell line were considered to be expressed in similar amounts in the two cell lines and therefore little or no affected by ERAP1/ERAP2; peptides with  $IR > 1.5$  in one cell line relative to the other, including peptides found only in that cell line, were considered to be up-regulated in that cell line and consequently

influenced by the ERAP1/ERAP2 context. The relationship of this classification to the statistical significance of the differences in peptide amounts was established by means of Volcano plots for each pairwise comparison (**Figure S2**). The alterations in the HLA-B\*51 peptidome were assessed by comparing the IR>1.5 peptide subsets from each cell line in each cell line pair. Analogous comparisons between the IR>1.0-1.5 subsets provided an internal control where the peptide changes due to ERAP1/2 should be attenuated or absent altogether.

The quantitative changes in the B\*51 peptidomes were assessed on the basis of the following features: 1) peptide length alterations, 2) P2 residue frequencies, which measures the alterations in the ratio of the two major subpeptidomes with Ala2 or Pro2, 3) changes in P1 residue frequencies within each subpeptidome, 4) differences in the frequencies of N-terminal flanking (P-1) residues, and 5) affinity differences.

The comparative analysis of the B\*51:01 peptidomes from a second 721.221-B\*51 transfectant and its shRNA-inhibited ERAP1 KO was carried out independently, but in an identical way.

## RESULTS

*Expression of ERAP1, ERAP2 and HLA-B\*51.* The presence or absence of ERAP1 and ERAP2 in 721.221-B\*51:01 and the various KO cells was confirmed by Western blot (**Figure 1A-B**). The effects of ERAP1 and/or ERAP2 depletion on the surface expression of B\*51:01 heterodimers and free heavy chains were assessed by flow cytometry with W6/32 and HC10, respectively (**Figure 1C-F**). The surface expression of HLA-B\*51 heterodimers was decreased by 30% to 50% in all the KO cell lines relative to the WT. In contrast, small or no differences in the expression of free MHC-I heavy chains were observed. As a result the folded/unfolded MHC-I ratio was highest in the WT and lowest in the E1E2KO cells. This result suggests that depleting ERAP1, ERAP2 or both enzymes leads to a globally less stable peptidome and lower B\*51:01 surface expression.

*Global effects of ERAP1 and ERAP2 depletion on the B\*51:01 peptidome.* A total of 2075 canonical and 485 non-canonical HLA-B\*51:01 ligands, which will be separately considered, were assigned from the 5 cell lines analyzed (**Table S1**). The numbers of canonical and non-

canonical peptides ranged from 1479 to 1747 and from 282 to 366, respectively, among individual cell lines (**Table 1**). A large majority of the peptides were shared among the various cell lines (**Figure S3**), indicating that most of the B\*51:01 ligands can be presented in the absence of ERAP1/2 processing.

The overall effects of ERAP1 and ERAP2 on the B\*51:01 peptidome were assessed by comparing the relative intensity of peptide subsets classified according to their length, P2 or PC motif (**Figure 2**). Nonamers were most abundant in the E2KO cells, which also showed the lowest amounts of 8-mers, whereas peptides >9-mers were most abundant in the E1E2KO cells. Moreover, E1E2KO cells showed the highest and lowest abundance of Ala2 and Pro2 peptides, respectively, whereas E2KO cells were equal to the WT in this feature. The relative abundance of peptides according to their PC residues showed only a marginal statistical significance, also observed between the two E1E2KO cell lines, suggesting that depletion of ERAP1 and/or ERAP2 has little global impact on this feature. These results indicate that ERAP1 and/or ERAP2 have an influence on peptide amounts beyond the limited qualitative effects on the presentation of individual ligands.

*Quantitative effects of ERAP1 and ERAP2 depletion on the B\*51:01 peptidome.* The availability of an ERAP1/ERAP2-positive cell line and the counterparts lacking one or both enzymes allowed us to define the effects of each enzyme on altering the amounts of HLA-B\*51 ligands according to their structural features by means of pairwise comparisons between appropriate cell lines. Thus, the effects of ERAP1 or ERAP2 depletion in the presence or absence of the other enzyme, as well as the effects of the joint depletion of both enzymes, could be separately established (**Table S2**). In each case the peptides from each cell line with IR>1.5 relative to the other (**Tables S3-S10**) were compared focusing on the following features: peptide length, frequency of Ala2 and Pro2, P1 residue frequencies among Ala2 and Pro2 peptides, since these are different in each subpeptidome (55), and PC residue usage. These comparisons are described in detail below and the results are summarized in **Table 2**. Pearson correlation analyses of the shared ligands between distinct cell lines showed that quantitative changes in the peptidome were much more drastic upon depletion of both enzymes than when only ERAP1 or

ERAP2 were knocked out (**Figure S4**), suggesting that the presence of only one of these enzymes was sufficient to carry out significant peptide processing in the ER.

*Quantitative effects of ERAP1 depletion.* The effects of ERAP1 depletion in the presence of ERAP2 were analyzed by comparing the B\*51:01 peptidomes from the 721.221-B\*51:01 WT with the E1KO cells. The following differences between the E1KO-derived peptides relative to the WT reached statistical significance in the IR>1.5 subsets (**Figure 3A**): 1) 9-mers were decreased whereas both 8-mers and peptides >9-mers were increased, 2) the abundance of peptides with Ala2 was increased and that of Pro2 peptides was decreased (Pro2/Ala2 ratio: 3.4-fold higher in the WT), 3) peptides with C-terminal Ile and Leu were increased to the expense of those with C-terminal Val. No statistically significant differences were observed in the frequency of P1 residues among either Ala2 or Pro2 peptides. Similar comparisons between the IR>1.0-1.5 subsets from both cell lines (**Figure S5A**) showed no statistically significant differences.

The effects of ERAP1 depletion in the absence of ERAP2 were analyzed by comparing the B\*51:01 peptidomes from the E2KO line with the E1E2KO lines #1 and #19 in the same way as above. When the IR>1.5 peptide subsets were compared (**Figure 3B-C**) the observed effects on peptide length, Pro2/Ala2 ratio and C-terminal residue usage were similar as those in the presence of ERAP2, although the difference in the Pro2/Ala2 ratio was larger (4.7-fold and 8.2-fold increased in the ERAP2 KO relative to the double KO clones #1 and 19 respectively) and those on PC frequencies were smaller. In addition, a statistically significant decrease in the frequency of Asp1, with a concomitant increase of Ser1 and Thr1, which reached statistical significance with E1E2 KO #1, was observed among Ala2 peptides. Yet, Asp1 was the most frequent P1 residue in this subpeptidome even in the absence of both ERAP1 and ERAP2. The decrease in Asp1 also reached statistical significance among the Pro2 peptides with E1E2KO #1. All these changes were attenuated or absent among the >1.0-1.5 subsets from both cell lines (**Figure S5B-C**). Although the same alterations were observed in the comparisons between E2KO and E1E2KO clones #1 and #19, the magnitude of the changes was somewhat different,

presumably reflecting clone-to-clone-differences unrelated to ERAP between both E1E2KO clones (**Figure S2**).

Thus, ERAP1 depletion has a profound effect on the B\*51:01 peptidome mainly on altering the relative abundance of Pro2 and Ala2 peptides, but also on peptide length and PC residue usage. These effects are largely independent of ERAP2, although the presence of this enzyme seems to attenuate these alterations to some extent.

To rule out that the alterations observed in the B\*51:01 peptidome were due to off-target effects in the CRISPR procedure, rather than to ERAP depletion, we performed an independent comparison using a distinct 721-221-B\*51:01 transfectant cell line and its shRNA-inhibited ERAP1KO, resulting in undetectable expression of the ERAP1 protein. A total of 1111 peptides, fulfilling the same stringent criteria described in previous paragraphs were considered as B\*51:01 ligands, of which 1074 and 665 were detected in the mock-inhibited control and the ERAP1KO, respectively. A comparison of the IR>1.5 peptide subsets from the mock and ERAP1-inhibited cells yielded very similar results as those obtained between the WT and CRISPR-generated ERAP1KO (**Figure S6**), strongly supporting that the peptidome changes in ERAP-KO cells should be considered the result of CRISPR on-targets effects.

*Quantitative effects of ERAP2 depletion.* The effects of ERAP2 depletion in the presence of ERAP1 were analyzed by comparing the B\*51:01 peptidomes from the WT and E2KO cells. The following differences between the E2KO-derived peptides with IR>1.5 relative to the IR>1.5 subset from the WT reached statistical significance (**Figure 4A**): 1) 9-mers and longer peptides were increased whereas 8-mers were decreased, 2) no effect on the Pro2/Ala2 subpeptidome balance was observed, but the frequency of Asp1 was decreased among Ala2 peptides and, without statistical significance, also in the Pro2 subpeptidome, 3) peptides with C-terminal Val were moderately decreased. A similar comparison between the IR>1.0-1.5 peptide subsets from both cell lines showed no statistically significant differences (**Figure S7A**).

The effects of ERAP2 depletion in the absence of ERAP1 were analyzed by comparing the B\*51:01 peptidomes from the E1KO line with the E1E2KO lines #1 and #19. When the IR>1.5 peptide subsets were compared (**Figure 4B-C**) the effects on peptide length were similar

but smaller than in the presence of ERAP1, involving an increased abundance of peptides >9-mers and a decrease of 8-mers, the latter reaching statistical significance only on E1E2KO #19 (**Figure 4C**). ERAP2 depletion in the absence of ERAP1 profoundly altered the Pro2/Ala2 ratio (2.6-fold and 4.8-fold increased in E1KO relative to E1E2KO #1 and 19, respectively), which is in contrast with the situation in the presence of this enzyme. The effects on P1 residue usage were similar, but larger, than in the presence of ERAP1: in the Ala2 subpeptidome the frequency of Asp1 was strongly decreased, whereas those of Ser1 and Thr1 were increased. The decrease of Asp1 was also observed in the Pro2 subpeptidome. C-terminal residue usage was little or no affected. No statistically significant effects were observed when comparing the IR>1.0-1.5 subsets from these cell lines (**Figure S7B-C**). As noted above, ERAP-unrelated clone-to-clone-differences probably account for the distinct magnitude of the effects observed between the comparisons of E1KO versus E1E2KO #1 and E1KO versus E1E2KO #19.

These results reflect a significant influence of ERAP2 on the B\*51:01 peptidome, which is distinct from that of ERAP1, but very dependent on the presence of this enzyme. They indicate that, in the absence of ERAP1, ERAP2 can process peptides in a way that is not apparent, or does not occur, in the presence of the former enzyme. The notorious influence of ERAP2 on the length of B\*51:01 ligands (**Figure 4A**) was attenuated in the absence of ERAP1 (**Figure 4B-C**), presumably because this enzyme favors the generation of 9-mers, which can be processed by ERAP2. The differential effects of ERAP2 on the Pro2/Ala2 balance, depending on the presence or absence of ERAP1 (**Figure 4**) demonstrate that the latter enzyme largely determines this balance, regardless of the presence of ERAP2. However, in the absence of ERAP1, the large influence of ERAP2 on the ratio between both subpeptidomes reveals that this enzyme can perform a redundant peptide processing function if ERAP1 is absent. The cleavage activity of ERAP2 is also reflected in the similar effects on P1 residue usage compared to those of ERAP1 depletion, which was most evident in the Ala2 subpeptidome (**Figures 3 and 4**).

*Quantitative effects of the joint depletion of ERAP1 and ERAP2.* The effects of the joint depletion of ERAP1 and ERAP2 were analyzed by comparing the B\*51:01 peptidomes from the WT and E1E2 KO #1 and #19, to account for ERAP-independent clone-to-clone-differences.

The following differences between the IR>1.5 subset from double KO-derived peptides relative to the IR>1.5 subset from the WT reached statistical significance (**Figure 5A-B**): 1) peptides >9-mers were increased and 9-mers were decreased, an effect similar to that observed upon ERAP1 depletion (**Figure 3**), except that the frequency of 8-mers was not affected, 2) peptides with Ala2 were increased and Pro2 peptides were decreased (Pro2/Ala2 ratio: 4.3-fold and 5.5-fold higher in the WT relative to KO cells #1 and #19, respectively), a pattern that was also similar to those upon ERAP1 depletion (**Figure 3**) or upon ERAP2 depletion in the absence of ERAP1 (**Figure 4B-C**), 3) the effects on P1 residue usage were also very similar to those observed upon depletion of either ERAP1 or ERAP2 in the absence of the other enzyme (**Figures 3B-C and 4B-C**), consisting in a strongly decreased frequency of Asp1 and increased frequency of Ser1 and Thr1 in the Ala2 subpeptidome, and a small but statistically significant decrease of Asp1 and increase of Arg1 in the Pro2 subpeptidome, and 4) peptides with C-terminal Val were decreased and those with C-terminal Leu were increased, which was again very similar to that obtained upon depletion of ERAP1 or ERAP2. Similar comparisons carried out between the IR>1.0-1.5 peptide subsets from these cell lines (**Figure S8**) showed no statistically significant differences.

Thus, most of the effects of the joint depletion of ERAP1 and ERAP2 on the B51:01 peptidome are very similar to those observed when single KO lines (E1KO or E2KO) were compared with E1E2KO cells. Therefore, the presence of a single enzyme, either ERAP1 or ERAP2, is sufficient for efficient processing of the B\*51:01 peptidome, confirming that ERAP2 can compensate to some extent for the absence of ERAP1.

The same analyses performed above (**Figures 3-5**) were also carried out with the more restricted sets of peptides statistically increased in each cell line in the volcano analyses plus those found only in that cell line of the two compared. The results obtained with this second approach (**Figures S9-S11**) closely reproduced the previous one, underlying the reliability of our IR classification criteria for assessing peptidome alterations between cell lines.

*Effects of ERAP1 and ERAP2 depletion on processing precursors of B\*51:01 ligands.* Next, we evaluated the effects of ERAP1 and/or ERAP2 on the type of precursors of B\*51 ligands that



are preferentially processed, by analyzing the frequencies of N-terminal flanking (P-1) residues, based on the comparison of the IR>1.5 peptide subsets from cell line pairs. The results are summarized in **Table 3**.

ERAP1 depletion in the presence of ERAP2 (WT vs E1KO) resulted in increased abundance of B\*51 ligands with Phe and Pro and decreased of those with Gly residues at P(-1). ERAP1 depletion in the absence of ERAP2 (E2KO vs E1E2KO) also resulted in a diminishment of small residues and increased Arg and hydrophobic ones. This pattern did not correlate with ERAP1 susceptibility, since both ERAP1-susceptible (i.e. Leu) and ERAP1-resistant residues (i.e Arg or Pro) were increased.

ERAP2 depletion in the presence of ERAP1 (WT vs ERAP2 KO) mainly resulted in decreased processing of peptide precursors with P(-1) basic residues. This result strongly suggests that ERAP2 can efficiently generate B\*51 ligands with ERAP2-susceptible P(-1) residues, revealing a direct role of this enzyme in epitope generation. ERAP2 depletion in the absence of ERAP1, (E1KO vs E1E2KO) resulted in increased abundance of B\*51 ligands with hydrophobic P(-1) residues at the expense of those with small ones. This pattern is very similar to that involving the joint depletion of both enzymes (WT vs E1E2KO), suggesting that ERAP2 can partially compensate for the absence of ERAP1 in the generation of B\*51:01 ligands. In addition, the fact that the pattern of P(-1) alterations bears no obvious correlation with ERAP1 or ERAP2 susceptibility suggests that, in the absence of these enzymes, the B\*51:01 peptidome is mainly composed of ligands that have been directly generated in the cytosol or in the ER by peptidases unrelated to ERAP1/2. No statistical differences were observed among the IR>1.0-1.5 subsets in any of the comparisons.

*The basis for the subpeptidome-dependent P1 residue usage among B\*51:01 ligands.* The predominance of Asp1 in the Ala2 subpeptidome, even in E1E2KO cells, cannot be explained solely by the resistance of this residue to ERAP1/2. We considered the possibility that the relative contribution of Asp and Leu at P1, the latter residue being predominant among Pro2 peptides, on B\*51 binding might depend on the P2 residue. Thus, we synthesized two series of four peptides each, consisting in two natural B\*51 ligands, DAYETTLHV and LPPVVAKEI

and 3 peptide variants of each of them, in which the two first residues were changed to generate the DA, LA, LP, DP combinations (**Table S11**), and tested their binding to B\*51:01 in an epitope stabilization assay (**Figure 6**). The experimental binding of the LPYETTLHV and DPYETTLHV showed that Leu1 and Asp1 were essentially equivalent for this peptide (EC50: 46 and 48  $\mu$ M, respectively). In contrast, binding of the LAYETTLHV and DAYETTLHV revealed that Asp1 was significantly better (EC50: 49 and 340  $\mu$ M for Asp1 and Leu1, respectively). A similar, but less dramatic, situation was obtained with the other peptide series. LPPVVAKEI showed a better binding than DPPVVAKEI (EC50: 33 and 74  $\mu$ M, respectively). In contrast, DAPVVAKEI showed a better binding than LAPVVAKEI (EC50: 58 and 77  $\mu$ M, respectively).

Thus, the relative contribution of Leu and Asp at P1 to B\*51:01 binding depends on the nature of the P2 residue, and also on the particular peptide sequence. These results suggest that the predominance of Asp1 in the Ala2 subpeptidome is at least partially explained by the binding features of Asp1 in an Ala2 context.

*Effects of ERAP1 and ERAP2 depletion on the affinity of the B\*51:01 peptidome.* The obvious lack of correlation between the experimental binding data and the theoretical affinity observed with these peptides (**Table S11**) suggests that the interactive effect of the P1 and P2 residues on B\*51:01 binding was not taken into account in the predictive algorithm used in this study, which might lead to an underestimation of the theoretical affinity of the Ala2 subpeptidome. Thus, we calculated the theoretical affinity of the peptides with Asp1 or other P1 residues among B\*51:01 ligands with Ala2 (**Figure S12**). The predicted affinity of the Ala2 peptides lacking Asp1 was higher compared to the whole Ala2 subpeptidome, but still lower than for Pro2 peptides. Since Asp1 accounts for a significant fraction of the Ala2 subpeptidome, the global affinity differences between the Pro2 and Ala2 subpeptidomes are probably smaller than those reflected by the theoretical algorithm.

Although the affinity differences between both subpeptidomes may not be properly quantified by the theoretical algorithm used in this study, this algorithm correctly predicts that Pro2 peptides have higher affinity than those with Ala2, since this is in agreement with

experimental binding data (70). Thus, it is possible to estimate the relative effects of ERAP1 and ERAP2 depletion on the affinity of the B\*51:01 peptidome based mainly on the effects of these enzymes on the Pro2/Ala2 ratio described above for the IR>1.5 subsets in pairwise comparisons. An additional effect on the affinity of the Ala2 subpeptidomes in these subsets is due to the changes in the Asp1 frequencies induced upon depletion of these enzymes, since Asp1 is a favored anchor for peptides with Ala2. Thus, a lower frequency of Asp1 among Ala2 peptides implies a lower affinity of this subpeptidome. The effects on both Pro2/Ala2 ratio and on the frequency of Asp1 in the Ala2 subpeptidome described in previous paragraphs are summarized in **Table S12**. Based on these values the effects of ERAP1/2 depletion on the affinity of the B\*51:01 peptidome may be ranked as follows: WT>E2KO>E1KO>E1E2KO.

*Effects of ERAP1 and ERAP2 depletion on presentation of non-canonical B\*51:01 ligands.* We next addressed the possibility that ERAP1 and/or ERAP2 depletion might increase the presentation of non-canonical B\*51:01 ligands, which accounted for about 15 to 19% of the B\*51:01 ligands identified in the various cell lines (**Table 1**). We designated as non-canonical ligands those showing only the canonical P2 motif (Pro2 or Ala2), or only the canonical PC motif (Ile, Leu, Val). Whereas the frequency of peptides with non-canonical PC residues was essentially the same in all cell lines, the frequency of peptides with non-canonical P2 residues was smaller in the WT compared to E1E2KO cells and in E2KO compared with E1E2KO #19 (**Figure 7**). Thus, in the absence of ERAP1 and ERAP2, B\*51:01 moderately increases the binding of peptides lacking an optimal P2 residue but maintaining an optimal PC anchor.

*How many peptides are altered upon ERAP1/ERAP2 depletion?* From the data presented in previous paragraphs it is possible to estimate the percentage of the B\*51:01 peptidome altered by ERAP1 and ERAP2. A global estimation can be directly obtained from the percentage of peptides showing statistically significant differences in expression in the volcano analyses between cell line pairs (**Figure S2**), taking into account that in these analyses peptides found only in one of the cell lines compared, or those found only in one of the three biological triplicates in any of the two cell lines, are not included. ERAP1 or ERAP2 depletion in the presence of the other enzyme (WT vs E1KO and WT vs E2KO) resulted in alterations of about

25% of the peptidome, whereas depletion of both enzymes (WT vs E1E2KO) affected about 40-50% of the peptidome. Since the E1E2 #1 vs #19 comparison yielded about 12% differences in this analysis, this value may be taken as a background of cell-to-cell differences unrelated to ERAP1/2 (**Table 4**).

In addition, the number of peptides altered in a given feature can be calculated from the percentage of alterations in that feature within the IR>1.5 subsets (also including the peptides found only in one of the two cell lines compared), assuming that the peptides within the IR>1.0 to 1.5 subsets are essentially unaltered by ERAP1/2. These estimations are also given in **Table 4** for alterations in P2 usage, peptide length and PC usage, but further effects occurred, for instance, in P1 usage within the Ala2 subpeptidome. This second approach shows that the effect of ERAP1/2 may be larger on one feature, such as P2 usage, than in another, such as length or C-terminal usage. Based on these estimations, the effects of ERAP1 and/or ERAP2 on P2 usage range from about 20% (WT/E1KO) to 30-40% (comparisons involving E1E2KO) of the peptidome, except in the WT/E2KO comparison, where essentially no effect on P2 usage was observed. Alterations in peptide length ranged from about 4% to 18.5% of the peptidome, the highest effect being observed in the WT/E2KO comparison. Alterations in PC usage ranged from 3.5% (E1KO/E1E2KO) to about 14% (WT/E1KO).

Although the data from both approaches cannot be directly compared because they address different features, the extent of the alterations in the peptidome are entirely consistent with each other and show that a significant fraction of the peptidome is altered at multiple levels by ERAP1 and ERAP2. Yet, about 50% of the peptidome remains apparently unaffected by ERAP1 and ERAP2, consistent with previous estimations (77,78)

## DISCUSSION

Two main issues were addressed in this study: dissecting the role of ERAP1 and ERAP2 in antigen processing, particularly in shaping the B\*51:01 peptidome, and correlating the changes induced by each of these enzymes with their association (ERAP1) or not (ERAP2) with Beçhet's disease. To approach these questions we analyzed the changes induced in the B\*51:01

peptidome from an ERAP1/ERAP2-positive cell line after knocking out either or both of these enzymes. The probability of off-target effects is reduced with the electroporation of the Cas9 ribonucleoprotein, as done in this study, because, in contrast to conventional DNA transfection, the editing machinery is degraded a few hours after entering the cell (79,80). To rule out off-target effects of the CRISPR as causative of the alterations observed, we demonstrated that the same changes in the B\*51:01 peptidome occurred upon ERAP1 depletion on an independently generated 721.221-B\*5:01 transfectant cell line where ERAP1 was depleted with shRNA. Since ERAP1 is expressed in all individuals whereas ERAP2 is not expressed in about 25% of the population (26), the peptidome of ERAP2 KO cells approaches a natural situation present in many individuals. In contrast, ERAP1-negative cells do not exist in normal individuals, although they may arise in tumors (81,82). The most similar physiological situation would be the homozygosity for the low activity variant Hap10/Hap10, a rare condition in human populations. Based on a survey of distinct ethnic groups from the 1000 genome program homozygous Hap10/Hap10 individuals (based on rs2287987), accounted for 1.7% (42 of 2504 individuals), of which only 0.3% (7 of 2504 individuals) were also ERAP2-negative (based on rs2248374). The very low frequency of Hap10/Hap10, ERAP2-negative individuals suggests that low ERAP1 activity in the absence of ERAP2 is biologically disfavored.

Our results allowed us to directly address the role of ERAP2 in the absence of ERAP1 and revealed several important aspects concerning the relationship between both enzymes in antigen processing: 1) lack of only ERAP2 induces significant changes in the B\*51:01 peptidome, implying that individuals expressing both enzymes present distinct peptidomes compared to those expressing only ERAP1, 2) in the absence of ERAP1, ERAP2 can carry out a significant processing of B\*51:01 ligands, implying a substantial trimming function of this enzyme, independently of ERAP1, 3) although our results do not exclude a functional interaction of both enzymes in shaping the B\*51:01 peptidome, they do not support a scenario in which ERAP2 functions essentially by facilitating ERAP1 processing, but rather as a largely independent enzyme, as also suggested by studies on HLA-B\*27 and A\*29:02 (57-59).

Both the nature and the magnitude of the changes in the B\*51:01 peptidome induced upon depletion of each enzyme are substantially different. This was most dramatically revealed by the following observations: 1) the opposite effects of ERAP1 and ERAP2 on peptide length, shown with single KO cells, which implied a key role of ERAP2 in determining the high abundance of 8-mers and the contribution of ERAP1 on favoring 9-mers. This is consistent with the distinct substrate length preferences of both enzymes. Upon ERAP1 depletion, less 9-mers are generated but 8-mers can still be efficiently produced by ERAP2 in the ER, leading to increased amounts of 8-mers, relative to 9-mers, in the ERAP1 KO (WT vs E1KO); in the absence of ERAP2, 9-mers are efficiently produced by ERAP1, but generation of 8-mers by this enzyme is much less efficient than with ERAP2, resulting in a lower 8-mer/9-mer balance in the ERAP2 KO compared to the WT (WT vs E2KO); in the absence of both enzymes neither of these effects take place, resulting in little or no alteration of the 8-mer/9-mer ratio and an increase of longer peptides in the double KO cells (WT vs E1E2KO #1 and #19), 2) the significant alteration of the Pro2/Ala2 subpeptidome ratio upon depletion of ERAP1, but not of ERAP2, when the other enzyme was present, leading to a substantially higher effect of ERAP1 on the affinity of the B\*51:01 peptidome, 3) the distinct effects of ERAP1 and ERAP2 on the precursors of B\*51:01 ligands, as revealed by the patterns of P(-1) processing, particularly the decreased frequency of B\*51:01 ligands with P(-1) basic residues in E2KO cells, whereas depletion of only ERAP1 induced a totally unrelated alteration, and 4) the larger alterations in PC residue usage induced by ERAP1 compared with ERAP2. Since the preference of ERAP1 for hydrophobic PC residues in the substrate is similar for Ile, Val, and Leu (21), it is unlikely that the differential preferences of ERAP1 and ERAP2 for C-terminal hydrophobic residues may account for the observed patterns of PC residue usage. A more likely explanation is that the suboptimal processing of peptides in the ER in the absence of ERAP1 leads to a higher abundance of potential B\*51 ligands with C-terminal Leu, relative to Val or Ile, simply because Leu is more frequent in the human proteome. In the presence of ERAP1, ERAP2 depletion still allows for significant peptide processing in the ER and the alteration in PC usage are therefore smaller.

A very interesting outcome of our study is that it revealed a substantial capacity of ERAP2, particularly evident in the absence of ERAP1, on antigen processing, so that depleting ERAP1 still endows the ER with a significant aminopeptidase activity due to ERAP2. This was indicated, in particular, by the nature and magnitude of the differences observed in the B\*51:01 peptidome between E1KO and E1E2KO cells. Thus, when compared with double KOs, both the presence of only ERAP1 (E2KO vs E1E2KO), or only ERAP2 (E1KO vs E1E2KO) resulted in very similar effects on increasing the Pro2/Ala2 subpeptidome ratio, the abundance of peptides with Asp1 in the Ala2 subpeptidome, and the patterns of (P-1) residue frequencies. We should explain how ERAP2 can substitute to a significant extent for the absence of ERAP1 in spite of the specificity and substrate handling differences between both enzymes. A likely possibility is that the joint frequency of ERAP2-susceptible residues, such as basic ones, Ala, Met and Gln (23) in the human peptidome is sufficiently high to allow for the generation of a large number of MHC-I epitopes in the absence of ERAP1. In addition, it cannot be ruled out that ERAP2 may still be able to cleave other residues in live cells, even if such cleavage is hardly observed *in vitro*. In the presence of ERAP1, since the trimming of most residues is much more efficient, the redundant trimming by ERAP2 might be less relevant, except for basic residues. The relevance of the functional redundancy of ERAP2 for non-B\*51:01 MHC-I peptidomes remains to be analyzed, but it may well be different depending on the particular binding preferences of each MHC-I molecule.

We previously proposed that the distinct P1 residue usage between the Pro2 and Ala2 subpeptidomes of B\*51:01 was determined by the inability of ERAP1/2 to cleave X-Pro, but not X-Ala bonds. In the former subpeptidome, P1 frequencies would be mainly determined by the binding preferences of B\*51:01, which favors hydrophobic P1 residues, and their frequency in the human peptidome, whereas ERAP1-mediated over-trimming of Ala2 ligands would lead to a predominance of the ERAP1-resistant Asp1 in this subpeptidome (55). Based on this assumption, the fact that the distinct patterns of P1 usage between both subpeptidomes were maintained, not only in the absence of ERAP1, but even in the absence of both ERAP1 and ERAP2, came as a surprise to us. This paradox is probably explained by the finding that the

relative contribution of Leu1 and Asp1 to B\*51:01 binding *in vitro* was reversed depending on the P2 residue, so that Asp1 was better anchor than Leu1 in an Ala2 context, and the opposite was true for Pro2 ligands. Yet, a substantial contribution of ERAP1/2 over-trimming to shaping the Ala2 subpeptidome is by no means excluded, and is actually supported by the much lower predominance of Asp1 in the double E1E2KO cells.

The basis for the increased preference of Asp1 in the Ala2 context for B\*51:01 binding is not fully clear to us. It was previously proposed that the unusual His171 residue in B\*51:01 may favor both negatively charged and hydrophobic residues at P1 (54). His171 is unusual among MHC-I molecules and provides a nonstandard anchorage of the P1 residue, whose detailed interaction pattern depends on the nature of this residue (71). It is likely that the peptidic Asp1 is stabilized through an interaction with the Arg62 residue in B\*51:01, similarly as Thr1 in the crystal structure of the TAFTIPSI/B\*51:01 complex (71). Indeed, Thr1 and Ser1 were, besides Asp1, among the predominant residues in the Ala2 subpeptidome upon depletion of both ERAP1 and ERAP2 in E1E2KO cells. It is possible that the structural rigidity of the X/Pro2 bond, compared with X/Ala2, may decrease the capacity of Asp1 to establish an optimal interaction with Arg62 and stabilize P1 anchoring in this way. A definitive assessment of this issue may require a crystallographic analysis of appropriate peptide/B\*51 complexes.

The high overlap between the peptidomes from WT and double KO cells implies that many B\*51:01 ligands can enter the ER in their final form and are available in the absence of ERAP1/2 processing. This applies also to those with disfavored TAP binding motifs, such as Asp1 or Pro2. Indeed, direct import of a B\*51 ligand with Pro2 generated in the cytosol into the ER was strongly suggested by a previous study (83). Nonetheless, the quantitative differences between these peptidomes indicate that B\*51:01 ligands also enter the ER as N-terminally extended precursors and are processed by ERAP1 and/or ERAP2, leading to both ligand generation, e.g. Pro2 ligands, which are overrepresented in the WT, and destruction, e.g. Ala2 ligands, which are underrepresented in the WT.

In spite of the substantial effects of ERAP1 and ERAP2 on peptide amounts, the basic structure of the B\*51 peptidome is fundamentally determined by the binding preferences of



B\*51. This was particularly evident in the small alterations in peptide length distribution, the maintenance of the subpeptidome structure, both in their distinct P1 and P2 motifs, the conservation of the PC motif, and the moderate increase of non-canonical peptides with suboptimal P2 residues. Thus, already formed ligands entering the ER provide a largely canonical HLA-B\*51 peptidome that obviates ERAP1/ERAP2 processing. This was also supported by the pattern of P(-1) usage in the absence of both enzymes and is consistent with the observation in this and other studies (77) that many peptides are unaffected, even in their expression levels, by ERAP1/ERAP2 silencing. This may reflect that there is an excess of preformed ligands in the ER (84), or that a number of peptides are either not processed by these enzymes or their generation/destruction balance results in unaltered peptide levels (38). Yet the B\*51:01 peptidome is optimized by ERAP1 and ERAP2, as revealed by its increased affinity and higher HLA-B\*51 surface expression on WT cells.

The effects of ERAP1/ERAP2 depletion on decreasing the surface expression of B\*51:01 are unlikely due to off-target effects since they were observed in the independently generated E1KO and E2KO cells. Our results are analogous to the decreased H-2K<sup>b</sup> expression upon ERAAP KO in mice (85), but differ from the unaltered expression of HLA-B\*27 heterodimers in ERAP1-depleted cells (77,86). This might be explained by the different HLA molecules involved and, in particular, by the lower affinity of B\*51:01 peptide complexes compared to HLA-B\*27 (55). Our results also differ from those in another study using the monocytic cell line U937 (87), where HLA-B\*51 expression was not affected by ERAP1 silencing. This apparent discrepancy must be assessed with caution since it might be due to the different ERAP1 silencing procedures or cell lines involved in both studies.

A second issue concerns the relevance of our study to understand the basis for the epistatic association of ERAP1 with Behçet's disease (41) and the apparent lack of association of ERAP2 with this disorder. Although other alternatives are not ruled out, it is reasonable to assume that the genetic relationship between these enzymes and Behçet's disease should be related to their antigen processing features and, in particular, to their effects on the peptidome of the major risk factor, B\*51:01. Indeed, polymorphic residues of this molecule critically

involved in determining its peptide-binding specificity showed association with Behçet's disease (88).

As demonstrated in this study and summarized above, both ERAP1 and ERAP2 have significant, but different effects, on the B\*51 peptidome, and these differences reflect largely separate actions on peptide trimming. Two of these differential features might be related to the differential association of ERAP1 and ERAP2 with Behçet's disease. The most obvious one is that disease susceptibility may be related to a differentially processed peptide, either one that is selectively generated or selectively destroyed by ERAP1, and is not dependent on ERAP2. Compelling evidence for such a peptide is missing, although antigen-specific CTL have been reported in Behçet's disease (48,89). This possibility is supported by the fact that, at least in the presence of ERAP1, the epitope generating-activity of ERAP2 is most conspicuous on peptide precursors with P(-1) basic residues, whereas ERAP1 has a much wider scope. In addition, over-trimming of B\*51:01 ligands with Ala2 should be predominantly carried out by ERAP1, due to its preference for hydrophobic P1 residues, which are good anchors for B\*51:01 (90). Over-trimming of basic P1 residues by ERAP2 is irrelevant since these are virtually absent in the B\*51:01 peptidome.

A second difference between ERAP1 and ERAP2 concerns their effects on the global affinity of the peptidome. Due to the likely limitation of the predictive algorithm already discussed, we cannot quantify affinity differences among B\*51:01 ligands. However, since Pro2 peptides have higher affinity (55,70), these differences are mainly related to the Pro2/Ala2 ratio, which was significantly affected by ERAP1. It was previously shown that this enzyme influences NK cell function by modulating the engagement of inhibitory KIR receptors in an affinity-dependent way (91), so that a peptidome with lower affinity might favor NK-mediated killing. Since NK cells have been implicated in Behçet's disease (49-51), the influence of ERAP1 on increasing the affinity of the B\*51:01 peptidome might be a mechanism influencing the association of this enzyme with Behçet's disease. It is important to note that the risk ERAP1 haplotype for this disease is the low activity Hap10 (42), which leads to a peptidome with lower

affinity (68) and potentially higher NK-activating capacity. Although ERAP2 also influenced the affinity of the B\*51:01 peptidome, its effect was substantially lower.

Thus, the distinct effects of ERAP1 and ERAP2 on the generation and destruction of peptide epitopes and on the affinity of the peptidome provide a sound basis for explaining the differential association of both enzymes with Behçet's disease through a distinct influence on the B\*51:01 peptidome: ERAP1-dependent changes, rather than those due to ERAP2, would influence diseases susceptibility, at least in HLA-B\*51-positive individuals.

It is possible that ERAP1-induced alterations in the peptidome of non-classical MHC-I molecules, such as HLA-E and/or HLA-G might influence NK recognition of these molecules, both of which have been reported to influence Behçet's disease susceptibility (92), as observed by the alterations in the peptidome of non-classical MHC-I molecules in ERAAP KO mice (93). Yet, this putative effect does not explain the epistatic association of ERAP1 and HLA-B\*51:01 with this disease.

This study follows those on HLA-B\*27 and A\*29:02 in examining the effects of ERAP1 and ERAP2 on the peptidomes of MHC-I molecules associated with inflammatory diseases (38). These studies yielded results that are consistent with the known features of both enzymes and reflect their processing role in the ER, which is common for all MHC-I ligands. Yet, their effects on each of the peptidomes analyzed are different, due to the distinct peptide pools selected for binding by each MHC-I molecule. This can explain both the different patterns of genetic associations of ERAP1 and ERAP2 and the different pathological features among MHC-I-associated diseases.

*Acknowledgements.* Supported by grants SAF2017/86578-R (Plan Nacional de I+D+i) to JALC, Israel Science Foundation, grant N. 1435/16 to AA, and an institutional grant of the Fundación Ramón Areces to the Centro de Biología Molecular *Severo Ochoa*. DF is supported by grants from the Italian Ministry of Health (PE-2011-02351866) and the Associazione Italiana Ricerca sul Cancro (AIRC: grant N. 18495). JJWK is supported by a VENI award from the Netherlands Organization for Scientific Research (N.W.O. project number 016.186.006). PG and EL are recipients of FPI (BES-2015-072729) and Juan de la Cierva (FJCI-2016-28335) awards from the Government of SPAIN, respectively. We thank Prof. Masafumi Takiguchi (Center for AIDS Research, Kumamoto University, Kumamoto, Japan) for kindly providing HLA-B\*51:01 transfectant cells and Sanne Hiddingh (Laboratory of Translational Immunology, University Medical Center, Utrecht University, The Netherlands) for her technical support in the generation of the KO cell lines.

*Data availability.* The mass spectrometry proteomics data have been deposited to the ProteomeXchange Consortium via the PRIDE partner repository (<http://www.ebi.ac.uk/pride>) with the dataset identifier: PXD012348. Username: [reviewer52025@ebi.ac.uk](mailto:reviewer52025@ebi.ac.uk); password: yoaVvHGh and username: [reviewer32331@ebi.ac.uk](mailto:reviewer32331@ebi.ac.uk); password: zq9VPTHh.

## Reference List

1. Garboczi, D. N., P. Ghosh, U. Utz, Q. R. Fan, W. E. Biddison, and D. C. Wiley. 1996. Structure of the complex between human T-cell receptor, viral peptide and HLA-A2. *Nature* **384**, 134-141.
2. Jardetzky, T. 1997. Not just another Fab: the crystal structure of a TcR-MHC-peptide complex. *Structure*. **5**, 159-163.
3. Lanier, L. L. 1998. NK cell receptors. *Annu.Rev.Immunol.* **16**, 359-393.
4. Brooks, A. G., J. C. Boyington, and P. D. Sun. 2000. Natural killer cell recognition of HLA class I molecules. *Rev.Immunogenet.* **2**, 433-448.
5. Yewdell, J. W., L. C. Anton, and J. R. Bennink. 1996. Defective ribosomal products (DRiPs): a major source of antigenic peptides for MHC class I molecules? *J.Immunol.* **157**, 1823-1826.
6. Princiotta, M. F., D. Finzi, S. B. Qian, J. Gibbs, S. Schuchmann, F. Buttgerit, J. R. Bennink, and J. W. Yewdell. 2003. Quantitating protein synthesis, degradation, and endogenous antigen processing. *Immunity*. **18**, 343-354.
7. Momburg, F., J. J. Neefjes, and G. J. Hammerling. 1994. Peptide selection by MHC-encoded TAP transporters. *Curr.Opin.Immunol.* **6**, 32-37.
8. Tsujimoto, M. and A. Hattori. 2005. The oxytocinase subfamily of M1 aminopeptidases. *Biochim.Biophys.Acta* **1751**, 9-18.
9. Saric, T., S. C. Chang, A. Hattori, I. A. York, S. Markant, K. L. Rock, M. Tsujimoto, and A. L. Goldberg. 2002. An IFN-gamma-induced aminopeptidase in the ER, ERAP1, trims precursors to MHC class I-presented peptides. *Nat.Immunol.* **3**, 1169-1176.
10. Saveanu, L., O. Carroll, V. Lindo, M. Del Val, D. Lopez, Y. Lepelletier, F. Greer, L. Schomburg, D. Fruci, G. Niedermann, and P. M. Van Endert. 2005. Concerted peptide trimming by human ERAP1 and ERAP2 aminopeptidase complexes in the endoplasmic reticulum. *Nat.Immunol.* **6**, 689-697.
11. York, I. A., S. C. Chang, T. Saric, J. A. Keys, J. M. Favreau, A. L. Goldberg, and K. L. Rock. 2002. The ER aminopeptidase ERAP1 enhances or limits antigen presentation by trimming epitopes to 8-9 residues. *Nat.Immunol.* **3**, 1177-1184.
12. Goto, Y., A. Hattori, Y. Ishii, and M. Tsujimoto. 2006. Reduced activity of the hypertension-associated Lys528Arg mutant of human adipocyte-derived leucine aminopeptidase (A-LAP)/ER-aminopeptidase-1. *FEBS Lett.* **580**, 1833-1838.
13. The TASK and WTCCC2 Consortia. 2011. Interaction between ERAP1 and HLA-B27 in ankylosing spondylitis implicates peptide handling in the mechanism for HLA-B27 in disease susceptibility. *Nat.Genet.* **43**, 761-767.
14. Evnouchidou, I., R. P. Kamal, S. S. Seregin, Y. Goto, M. Tsujimoto, A. Hattori, P. V. Voulgari, A. A. Drosos, A. Amalfitano, I. A. York, and E. Stratikos. 2011. Cutting Edge: Coding single nucleotide polymorphisms of endoplasmic reticulum

- aminopeptidase 1 can affect antigenic peptide generation in vitro by influencing basic enzymatic properties of the enzyme. *J.Immunol.* **186**, 1909-1913.
15. Kochan, G., T. Krojer, D. Harvey, R. Fischer, L. Chen, M. Vollmar, F. von Delft, K. L. Kavanagh, M. A. Brown, P. Bowness, P. Wordsworth, B. M. Kessler, and U. Oppermann. 2011. Crystal structures of the endoplasmic reticulum aminopeptidase-1 (ERAP1) reveal the molecular basis for N-terminal peptide trimming. *Proc.Natl.Acad.Sci.U.S.A* **108**, 7745-7750.
  16. Martin-Esteban, A., P. Gomez-Molina, A. Sanz-Bravo, and J. A. Lopez de Castro. 2014. Combined Effects of Ankylosing Spondylitis-associated ERAP1 Polymorphisms Outside the Catalytic and Peptide-binding Sites on the Processing of Natural HLA-B27 Ligands. *J.Biol.Chem.* **289**, 3978-3990.
  17. Reeves, E., C. J. Edwards, T. Elliott, and E. James. 2013. Naturally Occurring ERAP1 Haplotypes Encode Functionally Distinct Alleles with Fine Substrate Specificity. *J.Immunol.* **191**, 35-43.
  18. Stamogiannos, A., D. Koumantou, A. Papakyriakou, and E. Stratikos. 2015. Effects of polymorphic variation on the mechanism of Endoplasmic Reticulum Aminopeptidase 1. *Mol.Immunol.* **67**, 426-435.
  19. Ombrello, M. J., D. L. Kastner, and E. F. Remmers. 2015. Endoplasmic reticulum-associated amino-peptidase 1 and rheumatic disease: genetics. *Curr.Opin.Rheumatol.* **27**, 349-356.
  20. Hearn, A., I. A. York, and K. L. Rock. 2009. The specificity of trimming of MHC class I-presented peptides in the endoplasmic reticulum. *J.Immunol.* **183**, 5526-5536.
  21. Chang, S. C., F. Momburg, N. Bhutani, and A. L. Goldberg. 2005. The ER aminopeptidase, ERAP1, trims precursors to lengths of MHC class I peptides by a "molecular ruler" mechanism. *Proc.Natl.Acad.Sci.U.S.A* **102**, 17107-17112.
  22. Tanioka, T., A. Hattori, S. Masuda, Y. Nomura, H. Nakayama, S. Mizutani, and M. Tsujimoto. 2003. Human leukocyte-derived arginine aminopeptidase. The third member of the oxytocinase subfamily of aminopeptidases. *J.Biol.Chem.* **278**, 32275-32283.
  23. Lopez de Castro, J. A., C. Alvarez-Navarro, A. Brito, P. Guasp, A. Martin-Esteban, and A. Sanz-Bravo. 2016. Molecular and pathogenic effects of endoplasmic reticulum aminopeptidases ERAP1 and ERAP2 in MHC-I-associated inflammatory disorders: Towards a unifying view. *Mol.Immunol.* **77**, 193-204.
  24. López de Castro, J. A. and E. Stratikos. 2018. Intracellular antigen processing by ERAP2: Molecular mechanism and roles in health and disease. *Hum.Immunol.* **In press**. doi: **10.1016/j.humimm.2018.11.001**.
  25. Evnouchidou, I., J. Birtley, S. Seregin, A. Papakyriakou, E. Zervoudi, M. Samiotaki, G. Panayotou, P. Giastas, O. Petrakis, D. Georgiadis, A. Amalfitano, E. Saridakis, I. M. Mavridis, and E. Stratikos. 2012. A common single nucleotide polymorphism in endoplasmic reticulum aminopeptidase 2 induces a specificity switch that leads to altered antigen processing. *J.Immunol.* **189**, 2383-2392.
  26. Andres, A. M., M. Y. Dennis, W. W. Kretzschmar, J. L. Cannons, S. Q. Lee-Lin, B. Hurle, P. L. Schwartzberg, S. H. Williamson, C. D. Bustamante, R. Nielsen, A. G.

- Clark, and E. D. Green. 2010. Balancing selection maintains a form of ERAP2 that undergoes nonsense-mediated decay and affects antigen presentation. *PLoS.Genet.* **6**, e1001157.
27. Vanhoof, G., F. Goossens, M. De, I. D. Hendriks, and S. Scharpe. 1995. Proline motifs in peptides and their biological processing. *FASEB J.* **9**, 736-744.
  28. Mpakali, A., P. Giastas, N. Mathioudakis, I. M. Mavridis, E. Saridakis, and E. Stratikos. 2015. Structural basis for antigenic peptide recognition and processing by ER aminopeptidase 2. *J.Biol.Chem.* **290**, 26021-26032.
  29. Kuiper, J. J., J. Van Setten, S. Ripke, S. R. Van 't, F. Mulder, T. Missotten, G. S. Baarsma, L. C. Francioli, S. L. Pulit, C. G. De Kovel, N. Dam-Van Loon, A. I. Den Hollander, P. H. Veld, C. B. Hoyng, M. Cordero-Coma, J. Martin, V. Llorenc, B. Arya, D. Thomas, S. C. Bakker, R. A. Ophoff, A. Rothova, P. I. de Bakker, T. Mutis, and B. P. Koeleman. 2014. A genome-wide association study identifies a functional ERAP2 haplotype associated with birdshot chorioretinopathy. *Hum.Mol.Genet.* **23**, 6081-6087.
  30. Herbort, C. P., Jr., C. Pavesio, P. LeHoang, B. Bodaghi, C. Fardeau, P. Kestelyn, P. Neri, and M. Papadia. 2017. Why birdshot retinochoroiditis should rather be called 'HLA-A29 uveitis'? *Br.J.Ophthalmol.* **101**, 851-855.
  31. Brewerton, D. A., F. D. Hart, A. Nicholls, M. Caffrey, D. C. James, and R. D. Sturrock. 1973. Ankylosing spondylitis and HL-A 27. *Lancet* **1**, 904-907.
  32. Schlosstein, L., P. I. Terasaki, R. Bluestone, and C. M. Pearson. 1973. High association of an HL-A antigen, W27, with ankylosing spondylitis. *N.Engl.J.Med.* **288**, 704-706.
  33. Henseler, T. and E. Christophers. 1985. Psoriasis of early and late onset: characterization of two types of psoriasis vulgaris. *J.Am.Acad.Dermatol.* **13**, 450-456.
  34. Gudjonsson, J. E., A. Karason, E. H. Runarsdottir, A. A. Antonsdottir, V. B. Hauksson, H. H. Jonsson, J. Gulcher, K. Stefansson, and H. Valdimarsson. 2006. Distinct clinical differences between HLA-Cw\*0602 positive and negative psoriasis patients--an analysis of 1019 HLA-C- and HLA-B-typed patients. *J.Invest Dermatol.* **126**, 740-745.
  35. Ohno, S., M. Ohguchi, S. Hirose, H. Matsuda, A. Wakisaka, and M. Aizawa. 1982. Close association of HLA-Bw51 with Behcet's disease. *Arch.Ophthalmol.* **100**, 1455-1458.
  36. Gul, A. and S. Ohno. 2012. HLA-B\*51 and Behcet Disease. *Ocul.Immunol.Inflamm.* **20**, 37-43.
  37. de Menthon, M., M. P. LaValley, C. Maldini, L. Guillevin, and A. Mahr. 2009. HLA-B51/B5 and the risk of Behcet's disease: a systematic review and meta-analysis of case-control genetic association studies. *Arthritis Rheum.* **61**, 1287-1296.
  38. Lopez de Castro, J. A. 2018. How ERAP1 and ERAP2 Shape the Peptidomes of Disease-Associated MHC-I Proteins. *Front Immunol.* **9**, 2463.
  39. Kuiper, J. J. W., J. Setten, M. Devall, M. Cretu-Stanku, S. Hiddingh, R. A. Ophoff, T. Missotten, M. Van Velthoven, A. I. Den Hollander, C. B. Hoyng, E. James, E. Reeves, M. Cordero-Coma, A. Fonollosa, A. Adán, J. Martin, B. P. Koeleman, J. H. de Boer, S. L. Pulit, A. Márquez, and T. Radstake. 2018. Functionally distinct



ERAP1 and ERAP2 are a hallmark of HLA-A29-(Birdshot) Uveitis. *Hum.Mol.Genet.* **27**, 4333-4343.

40. Strange, A., F. Capon, C. C. Spencer, J. Knight, M. E. Weale, M. H. Allen, A. Barton, G. Band, C. Bellenguez, J. G. Bergboer, J. M. Blackwell, E. Bramon, S. J. Bumpstead, J. P. Casas, M. J. Cork, A. Corvin, P. Deloukas, A. Dilthey, A. Duncanson, S. Edkins, X. Estivill, O. Fitzgerald, C. Freeman, E. Giardina, E. Gray, A. Hofer, U. Huffmeier, S. E. Hunt, A. D. Irvine, J. Jankowski, B. Kirby, C. Langford, J. Lascorz, J. Leman, S. Leslie, L. Mallbris, H. S. Markus, C. G. Mathew, W. H. McLean, R. McManus, R. Mossner, L. Moutsianas, A. T. Naluai, F. O. Nestle, G. Novelli, A. Onoufriadis, C. N. Palmer, C. Perricone, M. Pirinen, R. Plomin, S. C. Potter, R. M. Pujol, A. Rautanen, E. Riveira-Munoz, A. W. Ryan, W. Salmhofer, L. Samuelsson, S. J. Sawcer, J. Schalkwijk, C. H. Smith, M. Stahle, Z. Su, R. Tazi-Ahnini, H. Traupe, A. C. Viswanathan, R. B. Warren, W. Weger, K. Wolk, N. Wood, J. Worthington, H. S. Young, P. L. Zeeuwen, A. Hayday, A. D. Burden, C. E. Griffiths, J. Kere, A. Reis, G. McVean, D. M. Evans, M. A. Brown, J. N. Barker, L. Peltonen, P. Donnelly, and R. C. Trembath. 2010. A genome-wide association study identifies new psoriasis susceptibility loci and an interaction between HLA-C and ERAP1. *Nat.Genet.* **42**, 985-990.
41. Kirino, Y., G. Bertsias, Y. Ishigatsubo, N. Mizuki, I. Tugal-Tutkun, E. Seyahi, Y. Ozyazgan, F. S. Sacli, B. Erer, H. Inoko, Z. Emrence, A. Cakar, N. Abaci, D. Ustek, C. Satorius, A. Ueda, M. Takeno, Y. Kim, G. M. Wood, M. J. Ombrello, A. Meguro, A. Gul, E. F. Remmers, and D. L. Kastner. 2013. Genome-wide association analysis identifies new susceptibility loci for Behcet's disease and epistasis between HLA-B\*51 and ERAP1. *Nat.Genet.* **45**, 202-207.
42. Takeuchi, M., M. J. Ombrello, Y. Kirino, B. Erer, I. Tugal-Tutkun, E. Seyahi, Y. Ozyazgan, N. R. Watts, A. Gul, D. L. Kastner, and E. F. Remmers. 2017. A single endoplasmic reticulum aminopeptidase-1 protein allotype is a strong risk factor for Behcet's disease in HLA-B\*51 carriers. *Ann.Rheum.Dis.* **75**, 2208-2211.
43. Cortes, A., J. Hadler, J. P. Pointon, P. C. Robinson, T. Karaderi, P. Leo, K. Cremin, K. Pryce, J. Harris, S. Lee, K. B. Joo, S. C. Shim, M. Weisman, M. Ward, X. Zhou, H. J. Garchon, G. Chiocchia, J. Nossent, B. A. Lie, O. Forre, J. Tuomilehto, K. Laiho, L. Jiang, Y. Liu, X. Wu, L. A. Bradbury, D. Elewaut, R. Burgos-Vargas, S. Stebbings, L. Appleton, C. Farrah, J. Lau, T. J. Kenna, N. Haroon, M. A. Ferreira, J. Yang, J. Mulero, J. L. Fernandez-Sueiro, M. A. Gonzalez-Gay, C. Lopez-Larrea, P. Deloukas, P. Donnelly, P. Bowness, K. Gafney, H. Gaston, D. D. Gladman, P. Rahman, W. P. Maksymowych, H. Xu, J. B. Crusius, van der Horst-Bruinsma IE, C. T. Chou, R. Valle-Onate, C. Romero-Sanchez, I. M. Hansen, F. M. Pimentel-Santos, R. D. Inman, V. Videm, J. Martin, M. Breban, J. D. Reveille, D. M. Evans, T. H. Kim, B. P. Wordsworth, and M. A. Brown. 2013. Identification of multiple risk variants for ankylosing spondylitis through high-density genotyping of immune-related loci. *Nat.Genet.* **45**, 730-738.
44. Robinson, P. C., M. E. Costello, P. Leo, L. A. Bradbury, K. Hollis, A. Cortes, S. Lee, K. B. Joo, S. C. Shim, M. Weisman, M. Ward, X. Zhou, H. J. Garchon, G. Chiocchia, J. Nossent, B. A. Lie, O. Forre, J. Tuomilehto, K. Laiho, L. Jiang, Y. Liu, X. Wu, D. Elewaut, R. Burgos-Vargas, L. S. Gensler, S. Stebbings, N. Haroon, J. Mulero, J. L. Fernandez-Sueiro, M. A. Gonzalez-Gay, C. Lopez-Larrea, P. Bowness, K. Gafney, J. S. Gaston, D. D. Gladman, P. Rahman, W. P. Maksymowych, H. Xu, van der Horst-Bruinsma IE, C. T. Chou, R. Valle-Onate, M. C. Romero-Sanchez, I. M. Hansen, F. M. Pimentel-Santos, R. D. Inman, J. Martin, M. Breban, D. Evans, J. D. Reveille, T. H. Kim, B. P. Wordsworth, and M. A. Brown. 2015. ERAP2 is associated with



ankylosing spondylitis in HLA-B27-positive and HLA-B27-negative patients. *Ann.Rheum.Dis.* **74**, 1627-1629.

45. Tsoi, L. C., S. L. Spain, J. Knight, E. Ellinghaus, P. E. Stuart, F. Capon, J. Ding, Y. Li, T. Tejasvi, J. E. Gudjonsson, H. M. Kang, M. H. Allen, R. McManus, G. Novelli, L. Samuelsson, J. Schalkwijk, M. Stahle, A. D. Burden, C. H. Smith, M. J. Cork, X. Estivill, A. M. Bowcock, G. G. Krueger, W. Weger, J. Worthington, R. Tazi-Ahnini, F. O. Nestle, A. Hayday, P. Hoffmann, J. Winkelmann, C. Wijmenga, C. Langford, S. Edkins, R. Andrews, H. Blackburn, A. Strange, G. Band, R. D. Pearson, D. Vukcevic, C. C. Spencer, P. Deloukas, U. Mrowietz, S. Schreiber, S. Weidinger, S. Koks, K. Kingo, T. Esko, A. Metspalu, H. W. Lim, J. J. Voorhees, M. Weichenthal, H. E. Wichmann, V. Chandran, C. F. Rosen, P. Rahman, D. D. Gladman, C. E. Griffiths, A. Reis, J. Kere, R. P. Nair, A. Franke, J. N. Barker, G. R. Abecasis, J. T. Elder, and R. C. Trembath. 2012. Identification of 15 new psoriasis susceptibility loci highlights the role of innate immunity. *Nat.Genet.* **44**, 1341-1348.
46. Yin, X., H. Q. Low, L. Wang, Y. Li, E. Ellinghaus, J. Han, X. Estivill, L. Sun, X. Zuo, C. Shen, C. Zhu, A. Zhang, F. Sanchez, L. Padyukov, J. J. Catanese, G. G. Krueger, K. C. Duffin, S. Mucha, M. Weichenthal, S. Weidinger, W. Lieb, J. N. Foo, Y. Li, K. Sim, H. Liany, I. Irwan, Y. Teo, C. T. Theng, R. Gupta, A. Bowcock, P. L. De Jager, A. A. Qureshi, P. I. de Bakker, M. Seielstad, W. Liao, M. Stahle, A. Franke, X. Zhang, and J. Liu. 2015. Genome-wide meta-analysis identifies multiple novel associations and ethnic heterogeneity of psoriasis susceptibility. *Nat.Comm.* **6**, 6916.
47. Sakane, T., M. Takeno, N. Suzuki, and G. Inaba. 1999. Behcet's disease. *N.Engl.J.Med.* **341**, 1284-1291.
48. Yasuoka, H., Y. Okazaki, Y. Kawakami, M. Hirakata, H. Inoko, Y. Ikeda, and M. Kuwana. 2004. Autoreactive CD8+ cytotoxic T lymphocytes to major histocompatibility complex class I chain-related gene A in patients with Behcet's disease. *Arthritis Rheum.* **50**, 3658-3662.
49. Hamzaoui, K., K. Ayed, M. Hamza, and J. L. Touraine. 1988. Natural killer cells in Behcet's disease. *Clin.Exp.Immunol.* **71**, 126-131.
50. Suzuki, Y., K. Hoshi, T. Matsuda, and Y. Mizushima. 1992. Increased peripheral blood gamma delta+ T cells and natural killer cells in Behcet's disease. *J.Rheumatol.* **19**, 588-592.
51. Hasan, M. S., P. L. Ryan, L. A. Bergmeier, and F. Fortune. 2017. Circulating NK cells and their subsets in Behcet's Disease. *Clin.Exp.Immunol.* **188**, 311-322.
52. Evnouchidou, I., M. Weimershaus, L. Saveanu, and P. van Endert. 2014. ERAP1-ERAP2 Dimerization Increases Peptide-Trimming Efficiency. *J.Immunol.* **193**, 901-908.
53. Chen, H., L. Li, M. Weimershaus, I. Evnouchidou, P. van Endert, and M. Bouvier. 2016. ERAP1-ERAP2 dimers trim MHC I-bound precursor peptides; implications for understanding peptide editing. *Sci.Rep.* **6**, 28902.
54. Falk, K., O. Rotzschke, M. Takiguchi, V. Gnau, S. Stevanovic, G. Jung, and H. G. Rammensee. 1995. Peptide motifs of HLA-B51, -B52 and -B78 molecules, and implications for Behcet's disease. *Int.Immunol.* **7**, 223-228.

55. Guasp, P., C. Alvarez-Navarro, P. Gomez-Molina, A. Martin-Esteban, M. Marcilla, E. Barnea, A. Admon, and J. A. López de Castro. 2016. The peptidome of the Behcet's disease-associated HLA-B\*51:01 includes two sub-peptidomes differentially shaped by ERAP1. *Arthritis Rheumatol.* **68**, 505-515.
56. Abelin, J. G., D. B. Keskin, S. Sarkizova, C. R. Hartigan, W. Zhang, J. Sidney, J. Stevens, W. Lane, G. L. Zhang, T. M. Eisenhaure, K. R. Clauser, N. Hacohen, M. S. Rooney, S. A. Carr, and C. J. Wu. 2017. Mass Spectrometry Profiling of HLA-Associated Peptidomes in Mono-allelic Cells Enables More Accurate Epitope Prediction. *Immunity.* **46**, 315-326.
57. Martin-Esteban, A., P. Guasp, E. Barnea, A. Admon, and J. A. Lopez de Castro. 2016. Functional Interaction of the Ankylosing Spondylitis Associated Endoplasmic Reticulum Aminopeptidase 2 with the HLA-B\*27 Peptidome in Human Cells. *Arthritis Rheumatol.* **68**, 2466-2475.
58. Martin-Esteban, A., A. Sanz-Bravo, P. Guasp, E. Barnea, A. Admon, and J. A. Lopez de Castro. 2017. Separate effects of the ankylosing spondylitis associated ERAP1 and ERAP2 aminopeptidases determine the influence of their combined phenotype on the HLA-B\*27 peptidome. *J.Autoimmun.* **79**, 28-38.
59. Sanz-Bravo, A., A. Martin-Esteban, J. J. W. Kuiper, M. Garcia-Peydro, E. Barnea, A. Admon, and J. A. Lopez de Castro. 2018. Allele-specific alterations in the peptidome underlie the joint association of HLA-A\*29:02 and Endoplasmic Reticulum Aminopeptidase 2 (ERAP2) with Birdshot Chorioretinopathy. *Mol.Cell Proteomics* **17**, 1564-1577.
60. Shimizu, Y. and R. DeMars. 1989. Production of human cells expressing individual transferred HLA-A,-B,-C genes using an HLA-A,-B,-C null human cell line. *J.Immunol.* **142**, 3320-3328.
61. Guasp, P., C. Alvarez-Navarro, P. Gomez-Molina, A. Martin-Esteban, M. Marcilla, E. Barnea, A. Admon, and J. A. López de Castro. 2017. Heterozygosity of the 721.221-B\*51:01 Cell Line Used in the Study by Guasp et (Arthritis Rheumatol, February 2016). *Arthritis and Rheumatol.* **69**, 686.
62. Ljunggren, H. G. and K. Karre. 1985. Host resistance directed selectively against H-2-deficient lymphoma variants. Analysis of the mechanism. *J.Exp.Med.* **162**, 1745-1759.
63. Nakayama, S., G. Kawaguchi, S. Karaki, T. Nagao, H. Uchida, K. Kashiwase, T. Akaza, T. Nasuno, and M. Takiguchi. 1994. Effect of single amino acid substitution at residue 167 of HLA-B51 on binding of antibodies and recognition of T cells. *Hum.Immunol.* **39**, 211-219.
64. Garcia-Medel, N., A. Sanz-Bravo, D. Van Nguyen, B. Galocha, P. Gomez-Molina, A. Martin-Esteban, C. Alvarez-Navarro, and J. A. López de Castro. 2012. Functional Interaction of the Ankylosing Spondylitis-associated Endoplasmic Reticulum Aminopeptidase 1 Polymorphism and HLA-B27 in Vivo. *Mol.Cell Proteomics.* **11**, 1416-1429.
65. Vázquez, M. N. and Lopez de Castro J.A. 2005. Similar cell surface expression of  $\beta$ 2-microglobulin-free heavy chains by HLA-B27 subtypes differentially associated with ankylosing spondylitis. *Arthritis Rheum.* **52**, 3290-3299.

66. Barnstable, C. J., W. F. Bodmer, G. Brown, G. Galfre, C. Milstein, A. F. Williams, and A. Ziegler. 1978. Production of monoclonal antibodies to group A erythrocytes, HLA and other human cell surface antigens. New tools for genetic analysis. *Cell* **14**, 9-20.
67. Stam, N. J., H. Spits, and H. L. Ploegh. 1986. Monoclonal antibodies raised against denatured HLA-B locus heavy chains permit biochemical characterization of certain HLA-C locus products. *J.Immunol.* **137**, 2299-2306.
68. Guasp, P., E. Barnea, M. F. Gonzalez-Escribano, A. Jimenez-Reinoso, J. R. Regueiro, A. Admon, and J. A. Lopez de Castro. 2017. The Behcet's disease-associated variant of the aminopeptidase ERAP1 shapes a low affinity HLA-B\*51 peptidome by differential subpeptidome processing. *J.Biol.Chem.* **292**, 9680-9689.
69. Ishihama, Y., J. Rappsilber, J. S. Andersen, and M. Mann. 2002. Microcolumns with self-assembled particle frits for proteomics. *J.Chromatogr.A* **979**, 233-239.
70. Sakaguchi, T., M. Ibe, K. Miwa, Y. Kaneko, S. Yokota, K. Tanaka, and M. Takiguchi. 1997. Binding of 8-mer to 11-mer peptides carrying the anchor residues to slow assembling HLA class I molecules (HLA-B\*5101). *Immunogenetics* **45**, 259-265.
71. Maenaka, K., T. Maenaka, H. Tomiyama, M. Takiguchi, D. I. Stuart, and E. Y. Jones. 2000. Nonstandard peptide binding revealed by crystal structures of HLA-B\*5101 complexed with HIV immunodominant epitopes. *J.Immunol.* **165**, 3260-3267.
72. Bertoni, R., J. Sidney, P. Fowler, R. W. Chesnut, F. V. Chisari, and A. Sette. 1997. Human histocompatibility leukocyte antigen-binding supermotifs predict broadly cross-reactive cytotoxic T lymphocyte responses in patients with acute hepatitis. *J.Clin.Invest* **100**, 503-513.
73. Lorente, E., S. Infantes, E. Barnea, I. Beer, R. Garcia, F. Lasala, M. Jimenez, C. Vilches, F. A. Lemonnier, A. Admon, and D. Lopez. 2012. Multiple viral ligands naturally presented by different class I molecules in transporter antigen processing-deficient vaccinia virus-infected cells. *J.Virol.* **86**, 527-541.
74. Karosiene, E., C. Lundegaard, O. Lund, and M. Nielsen. 2012. NetMHCcons: a consensus method for the major histocompatibility complex class I predictions. *Immunogenetics* **64**, 177-186.
75. Cox, J. and M. Mann. 2008. MaxQuant enables high peptide identification rates, individualized p.p.b.-range mass accuracies and proteome-wide protein quantification. *Nat.Biotechnol.* **26**, 1367-1372.
76. Cox, J., N. Neuhauser, A. Michalski, R. A. Scheltema, J. V. Olsen, and M. Mann. 2011. Andromeda: a peptide search engine integrated into the MaxQuant environment. *J.Proteome.Res.* **10**, 1794-1805.
77. Barnea, E., K. D. Melamed, Y. Haimovich, N. Satumtira, M. L. Dorris, M. T. Nguyen, R. E. Hammer, T. M. Tran, R. A. Colbert, J. D. Taurog, and A. Admon. 2017. The HLA-B27 peptidome in vivo in spondyloarthritis-susceptible HLA-B27 transgenic rats and the effect of ERAP1 deletion. *Mol.Cell Proteomics* **16**, 642-662.
78. Admon, A. 2019. ERAP1 shapes just part of the immunopeptidome. *Hum.Immunol.* **doi: 10.1016/j.humimm.2019.03.004. [Epub ahead of print]**.

79. Kim, S., D. Kim, S. W. Cho, J. Kim, and J. S. Kim. 2014. Highly efficient RNA-guided genome editing in human cells via delivery of purified Cas9 ribonucleoproteins. *Genome Res.* **24**, 1012-1019.
80. Cho, S. W., S. Kim, Y. Kim, J. Kweon, H. S. Kim, S. Bae, and J. S. Kim. 2014. Analysis of off-target effects of CRISPR/Cas-derived RNA-guided endonucleases and nickases. *Genome Res.* **24**, 132-141.
81. Fruci, D., S. Ferracuti, M. Z. Limongi, V. Cunsolo, E. Giorda, R. Fraioli, L. Sibilio, O. Carroll, A. Hattori, P. M. Van Endert, and P. Giacomini. 2006. Expression of endoplasmic reticulum aminopeptidases in EBV-B cell lines from healthy donors and in leukemia/lymphoma, carcinoma, and melanoma cell lines. *J.Immunol.* **176**, 4869-4879.
82. Fruci, D., P. Giacomini, M. R. Nicotra, M. Forloni, R. Fraioli, L. Saveanu, P. van Endert, and P. G. Natali. 2008. Altered expression of endoplasmic reticulum aminopeptidases ERAP1 and ERAP2 in transformed non-lymphoid human tissues. *J.Cell Physiol* **216**, 742-749.
83. Levy, F., L. Burri, S. Morel, A. L. Peitrequin, N. Levy, A. Bachi, U. Hellman, B. J. Van den Eynde, and C. Servis. 2002. The final N-terminal trimming of a subaminoterminal proline-containing HLA class I-restricted antigenic peptide in the cytosol is mediated by two peptidases. *J.Immunol.* **169**, 4161-4171.
84. Komov, L., D. M. Kadosh, E. Barnea, E. Milner, A. Hendler, and A. Admon. 2018. Cell Surface MHC Class I Expression Is Limited by the Availability of Peptide-Receptive "Empty" Molecules Rather than by the Supply of Peptide Ligands. *Proteomics* **18**, e1700248.
85. Hammer, G. E., F. Gonzalez, E. James, H. Nolla, and N. Shastri. 2007. In the absence of aminopeptidase ERAAP, MHC class I molecules present many unstable and highly immunogenic peptides. *Nat.Immunol.* **8**, 101-108.
86. Chen, L., A. Ridley, A. Hammitzsch, M. H. Al Mossawi, H. Bunting, D. Georgiadis, A. Chan, S. Kollnberger, and P. Bowness. 2016. Silencing or inhibition of endoplasmic reticulum aminopeptidase 1 (ERAP1) suppresses free heavy chain expression and Th17 responses in ankylosing spondylitis. *Ann.Rheum.Dis.* **75**, 916-923.
87. Tran, T. M., S. Hong, J. H. Edwan, and R. A. Colbert. 2016. ERAP1 reduces accumulation of aberrant and disulfide-linked forms of HLA-B27 on the cell surface. *Mol.Immunol.* **74**, 10-17.
88. Ombrello, M. J., Y. Kirino, P. I. de Bakker, A. Gul, D. L. Kastner, and E. F. Remmers. 2014. Behcet disease-associated MHC class I residues implicate antigen binding and regulation of cell-mediated cytotoxicity. *Proc.Natl.Acad.Sci.U.S.A* **111**, 8867-8872.
89. Kaneko, S., N. Suzuki, N. Yamashita, H. Nagafuchi, T. Nakajima, S. Wakisaka, S. Yamamoto, and T. Sakane. 1997. Characterization of T cells specific for an epitope of human 60-kD heat shock protein (hsp) in patients with Behcet's disease (BD) in Japan. *Clin.Exp.Immunol.* **108**, 204-212.
90. Sakaguchi, T., M. Ibe, K. Miwa, S. Yokota, K. Tanaka, C. Schonbach, and M. Takiguchi. 1997. Predominant role of N-terminal residue of nonamer peptides in their binding to HLA-B\* 5101 molecules. *Immunogenetics* **46**, 245-248.

91. Cifaldi, L., P. Romania, M. Falco, S. Lorenzi, R. Meazza, S. Petrini, M. Andreani, D. Pende, F. Locatelli, and D. Fruci. 2015. ERAP1 regulates natural killer cell function by controlling the engagement of inhibitory receptors. *Cancer Res.* **75**, 824-834.
92. Park, K. S., J. S. Park, J. H. Nam, D. Bang, S. Sohn, and E. S. Lee. 2007. HLA-E\*0101 and HLA-G\*010101 reduce the risk of Behcet's disease. *Tissue Antigens* **69**, 139-144.
93. Nagarajan, N. A., D. A. de Verteuil, D. Sriranganadane, W. Yahyaoui, P. Thibault, C. Perreault, and N. Shastri. 2016. ERAAP Shapes the Peptidome Associated with Classical and Nonclassical MHC Class I Molecules. *J.Immunol.* **197**, 1035-1043.

**Table 1 - HLA-B\*51 ligands**

		<b>Canonical</b>		<b>Non-canonical</b>	
	<b>N. of peptides</b>	<b>Total</b>		<b>Total</b>	
	Total	N	%	N	%
<b>All</b>	<b>2560</b>	<b>2075</b>	<b>81.1</b>	<b>485</b>	<b>18.9</b>
WT	1888	1606	85.1	282	14.9
E1KO	1980	1644	83.0	336	17.0
E2KO	2076	1747	84.2	329	15.8
E1E2KO #1	1819	1479	81.3	340	18.7
E1E2KO #19	1944	1578	81.2	366	18.8

**Table 2. Summary of the effects observed on the HLA-B\*51:01 peptidome in pairwise comparisons among WT, E1KO, E2KO and E1E2KO cells**

Effects on	Effects of <sup>a</sup>				
	ERAP1 depletion		ERAP2 depletion		ERAP1+ERAP2 depletion
	WT/E1KO	E2KO/E1E2KO	WT/E2KO	E1KO/E1E2KO	WT/E1E2KO
<b>Length</b>					
8-mers	Up	Up	Down	Down	No effect
9-mers	Down	Down	Up	No effect	Down
>9-mers	Up	Up	Up	Up	Up
<b>Subpeptidomes</b>					
Ala2	Up	Up	No effect	Up	Up
Pro2	Down	Down	No effect	Down	Down
<b>P1 usage</b>					
Ala2	No effect	Asp: Down Thr/Ser: Up	Asp: Down	Asp: Down Thr/Ser: Up	Asp: Down Thr/Ser: Up
Pro2	No effect	Asp: down	No effect	Asp: Down Arg: Up	Asp: Down Arg: Up
<b>PC usage</b>					
Val	Down	Down	Down	No effect	Down
Leu + Ile	Up	Up	Up	No effect	Up

<sup>a</sup>Statistically significant changes. In the comparisons involving E1E2KO clonal lines, statistically significant changes observed with one of the clones were taken into account if the same tendency, although without statistical significance, was observed with the other clone. **P-values are given in Figures 3 to 5.**

**Table 3. Statistically increased P(-1) residues between B\*51:01 ligands with IR>1.5 from the indicated cell line pairs<sup>a</sup>.**

ERAP1 depletion (ERAP2+)		ERAP2 depletion (ERAP1+)		ERAP1 depletion (ERAP2-)		ERAP2 depletion (ERAP1-)		ERAP1+2 depletion	
WT	E1KO	WT	E2KO	E2KO	E1E2KO	E1KO	E1E2KO	WT	E1E2KO
G 0.03	F 0.02	R 1.8E-05		S 5.0E-11 8.6E-11	R 0.03 0.03	S 2.6E-07 3.8E-06	L 1.7E-09 1.7E-09	S 1.1E-05 1.3E-04	L 3.5E-07 2.0E-06
	P 0.03	K 5.3E-04		G 1.3E-03 2.0E-03	L 6.2E-05 1.7E-07	G 5.9E-05 5.6E-07	F 2.6E-06 4.4E-04	G 2.5E-07 3.5E-08	F 3.6E-05 3.5E-05
					F 3.4E-04 1.3E-03	A 7.6E-08 2.4E-10	Y 5.0E-03 0.03	A 0.02 6.5E-03	Y 0.02 0.02
					P 4.6E-06 5.0E-04		P 6.8E-05 4.4E-04		P 2.2E-06 2.2E-06

<sup>a</sup>Statistical significance was assessed with the  $\chi^2$  test with Bonferroni correction. Statistically significant p-values (<0.05) are indicated. In the comparisons involving E1E2KO #1 and #19 only those residues showing statistical significance with both clones were taken into account. The double p-values in these comparisons indicate the difference with clones #1 and #19 respectively.



**Table 4. Estimated extent of the alterations induced in the B\*51 peptidome by ERAP1 and/or ERAP2 depletion**

Role of	Comparisons	Volcano analyses <sup>a</sup>			Altered features <sup>b</sup>		P2		Length		PC	
		N	Significant	% Altered	Total	IR>1.5 ( $\Sigma$ )	$\Delta$ (%)	% altered	$\Delta$ (%)	% altered	$\Delta$ (%)	% altered
ERAP1 (E2+)	WT/E1KO	1127	284	25.2	1842	1364	27.7	<b>20.5</b>	14	<b>10.4</b>	19.2	<b>14.2</b>
ERAP1 (E2-)	E2KO/E1E2KO #1	1012	486	48.0	1925	1595	38.1	<b>31.6</b>	19	<b>15.7</b>	8.5	<b>7.0</b>
	E2KO/E1E2KO #19	1077	538	50.0	1948	1616	48.2	<b>40.0</b>	13.4	<b>11.1</b>	7.8	<b>6.5</b>
ERAP2 (E1+)	WT/E2KO	1188	301	25.3	1873	1193	N.S.	<b>N.S.</b>	29.1	<b>18.5</b>	12	<b>7.6</b>
ERAP2 (E1-)	E1KO/E1E2KO #1	1053	362	34.4	1808	1422	24.9	<b>19.6</b>	4.8	<b>3.8</b>	4.5	<b>3.5</b>
	E1KO/E1E2KO #19	1114	416	37.3	1843	1298	35.9	<b>25.3</b>	11.2	<b>7.9</b>	4.9	<b>3.5</b>
ERAP1+2	WT/E1E2KO #1	917	376	41.0	1888	1572	33.2	<b>27.6</b>	10.9	<b>9.1</b>	12.4	<b>10.3</b>
	WT/E1E2KO #19	962	439	45.6	1940	1574	41.5	<b>33.7</b>	5.5	<b>4.5</b>	11.3	<b>9.2</b>

<sup>a</sup>Volcano analyses (**Figure S2**): N, total peptides compared, including only peptides found in both cell lines and identified in more than one of the biological triplicates of each cell line; Significant and %altered indicate total peptides and percent relative to N, respectively, showing statistically significant expression differences between the cells compared. As a control, the % altered peptides between E1E2KO clones #1 and #19 in this comparison was to 12.3%.

<sup>b</sup>Altered features (**Figures 3-5**): Total, number of peptides shared between the two cell lines compared plus peptides found only in each one of the two cell lines; IR>1.5 ( $\Sigma$ ), added peptides from the IR>1.5 subsets from each cell line, including peptides found only in one of the cell lines;  $\Delta$  (%), percent of peptide differences found in the comparison between the IR>1.5 subsets, as shown in **Figures 3-5**. Only those features showing statistical significance were included. N.S.: not significant. % altered, % of the total peptidome altered in each given feature.

### FIGURE LEGENDS.

**Figure 1. ERAP1, ERAP2 and surface HLA-B\*51:01 expression.** Western blot of (A) ERAP1 and (B) ERAP2 expression in the indicated cell lines. Gamma-tubulin was used as a loading control. Expression of (C) folded HLA class I (W6/32) and (D) free heavy chain (HC10) relative to the WT in the indicated cell lines assessed by flow cytometry. Data are mean values  $\pm$  s.d. from 4 to 7 different experiments and statistically significant p-values, assessed with the Student's t test, are given. (E) Representative histograms of the surface expression of folded HLA class I and free heavy chain. (F) Folded/unfolded HLA (W6/32: HC10) ratio. The data were calculated as the ratio between the mean values in panels C and D.

**Figure 2. Global effects of ERAP1 and ERAP2 on the HLA-B\*51:01 peptidome.** Ion peak intensities relative to the total intensity of all the canonical peptides from the indicated cell lines (Peptide numbers are given in Table 1) were calculated and their values were grouped according to peptide length (upper panel), P2 residue (middle panel) and PC residue (bottom panel). The data are mean values and standard deviation of three independent experiments. Statistically significant differences were calculated using the Student's t-test and their p-values are shown.

**Figure 3. Effect of ERAP1 depletion on the HLA-B\*51:01 peptidome.** Comparison of the peptides with IR>1.5 from the indicated cell lines. These subsets include both shared peptides over-represented plus those found only in the corresponding cell line of the two being compared. The effects of ERAP1 depletion in (A) the presence of ERAP2 (WT vs E1KO, N: 721 and 643 peptides, respectively) or the absence of this enzyme (B) E2KO vs E1E2KO #1 (N: 910 and 685 peptides, respectively) and (C) E2KO vs E1E2KO #19 (N: 817 and 799 peptides, respectively) on peptide length (upper panels), P2 residue usage (second panels), P1 residue usage among peptides with Ala2 (third panels) or Pro2 (fourth panels), and PC residue usage (bottom panels) were assessed. Statistically significant differences were calculated using the  $\chi^2$  test with Bonferroni correction and their p-values are indicated. All other differences are not significant.

**Figure 4. Effect of ERAP2 depletion on the HLA-B\*51:01 peptidome.** Comparison of the peptides with IR>1.5 from the indicated cell lines were grouped as in Figure 3. The effects of

ERAP2 depletion in **(A)** the presence of ERAP1 (WT vs E2KO, N: 467 and 726 peptides, respectively) or the absence of this enzyme **(B)** E1KO vs E1E2KO #1 (N: 699 and 723 peptides, respectively) and **(C)** E1KO vs E1E2KO #19 (N: 613 and 865 peptides, respectively) on peptide length (upper panels), P2 residue usage (second panels), P1 residue usage among peptides with Ala2 (third panels) or Pro2 (fourth panels), and PC residue usage (bottom panels) were assessed. Statistically significant differences were calculated using the  $\chi^2$  test with Bonferroni correction and their p-values are indicated. All other differences are not significant.

**Figure 5. Effect of ERAP1 and ERAP2 depletion on the HLA-B\*51:01 peptidome.**

Comparison of the peptides with IR>1.5 from the indicated cell lines grouped as in Figure 3. The effects of ERAP1 and ERAP2 depletion in **(A)** clone #1 (WT vs E1E2KO #1, N: 887 and 757 peptides, respectively) or **(B)** clone #19 (WT vs E1E2KO #19, N: 817 and 866 peptides, respectively) on peptide length (upper panels), P2 residue usage (second panels), P1 residue usage among peptides with Ala2 (third panels) or Pro2 (fourth panels), and PC residue usage (bottom panels) were assessed. Statistically significant differences were calculated using the  $\chi^2$  test with Bonferroni correction and their p-values are indicated. All other differences are not significant.

**Figure 6. Epitope stabilization assay.** Surface stabilization of HLA-B\*51:01 by synthetic peptides corresponding to the natural ligands DAYETTLHV (upper panels) and LPPVVAKEI (lower panels) and their analogs with the following sequences at P1 and P2: LP, DP (left panels), LA and DA (right panels). The surface expression of HLA-B\*51:01 was measured by flow cytometry and represented as fold change relative to the fluorescence obtained with the B\*27 ligand KRLEEIMKR, used as negative control (C-). EC50 values were calculated as the peptide concentration that yielded 50% of the maximum stabilization obtained with the hepatitis B virus HBc19-27 peptide LPSDFFPSV used as positive control. Data are means  $\pm$  s.d. of three independent experiments.

**Figure 7. Effect of ERAP1 and ERAP2 on the presentation of non-canonical HLA-B\*51:01 ligands.** Peptides with non-canonical PC (filled bars) or P2 (checkered bars) residues in the indicated cell lines are shown as the percentage of the total peptides identified in the same cell

line. Statistically significant differences were calculated using the  $\chi^2$  test and their p-values are indicated. All other differences are not significant.

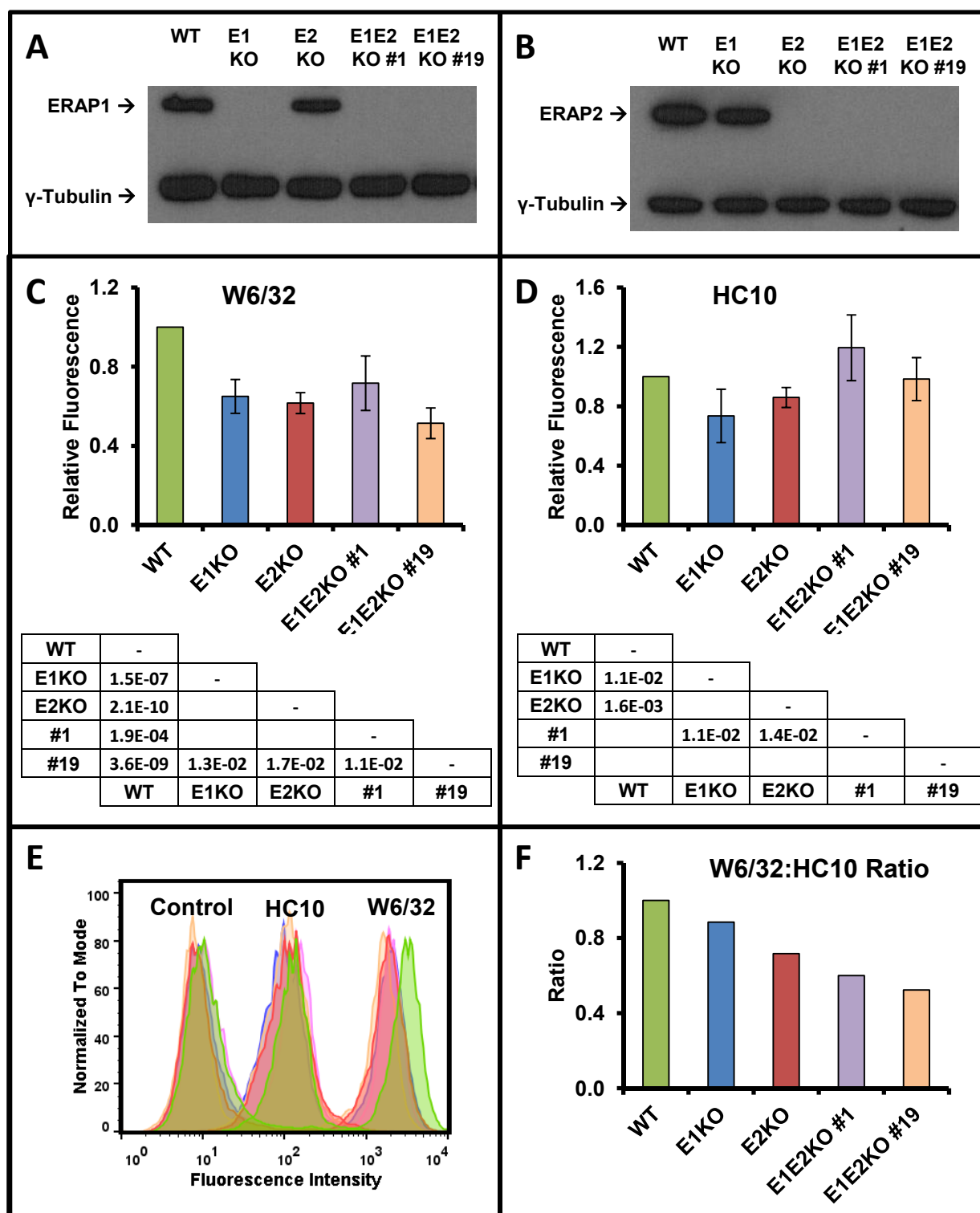
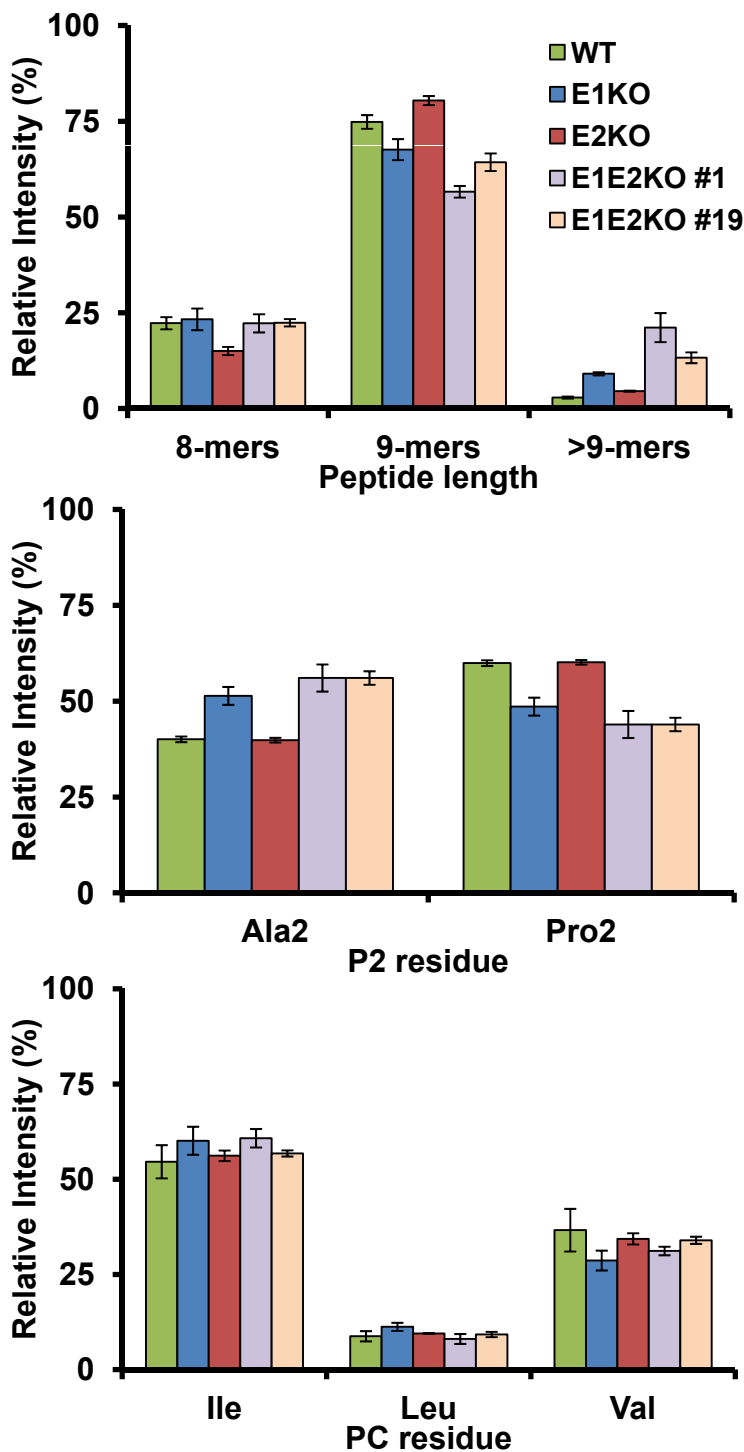


**Figure 1**



Statistically significant differences in relative intensity				
Peptide length				
8-mer	WT	E1KO	E2KO	E1E2KO 1
WT	-			
E1KO		-		
E2KO	2.8E-03	9.1E-03	-	
E1E2KO 1			8.5E-03	-
E1E2KO 19			8.8E-04	
9-mer	WT	E1KO	E2KO	E1E2KO 1
WT	-			
E1KO	1.9E-02	-		
E2KO	1.1E-02	1.7E-03	-	
E1E2KO 1	1.7E-04	3.7E-03	2.8E-05	-
E1E2KO 19	3.3E-03		4.1E-04	8.3E-03
>9-mer	WT	E1KO	E2KO	E1E2KO 1
WT	-			
E1KO	2.6E-05	-		
E2KO	6.7E-04	5.6E-05	-	
E1E2KO 1	1.1E-03	5.4E-03	1.6E-03	-
E1E2KO 19	2.3E-04	7.8E-03	4.3E-04	2.8E-02
Subpeptidomes				
	WT	E1KO	E2KO	E1E2KO 1
WT	-			
E1KO	1.3E-03	-		
E2KO		1.2E-03	-	
E1E2KO 1	1.5E-03		1.4E-03	-
E1E2KO 19	1.3E-04		1.1E-04	
PC usage				
Ile	WT	E1KO	E2KO	E1E2KO 1
WT	-			
E1KO		-		
E2KO			-	
E1E2KO 1			4.63E-02	-
E1E2KO 19				
Leu	WT	E1KO	E2KO	E1E2KO 1
WT	-			
E1KO		-		
E2KO		4.7E-02	-	
E1E2KO 1		3.1E-02		-
E1E2KO 19				
Val	WT	E1KO	E2KO	E1E2KO 1
WT	-			
E1KO		-		
E2KO		3.0E-02	-	
E1E2KO 1			4.0E-02	-
E1E2KO 19		2.9E-02		2.9E-02

**Figure 2**

ERAP1 depletion (IR>1.5)

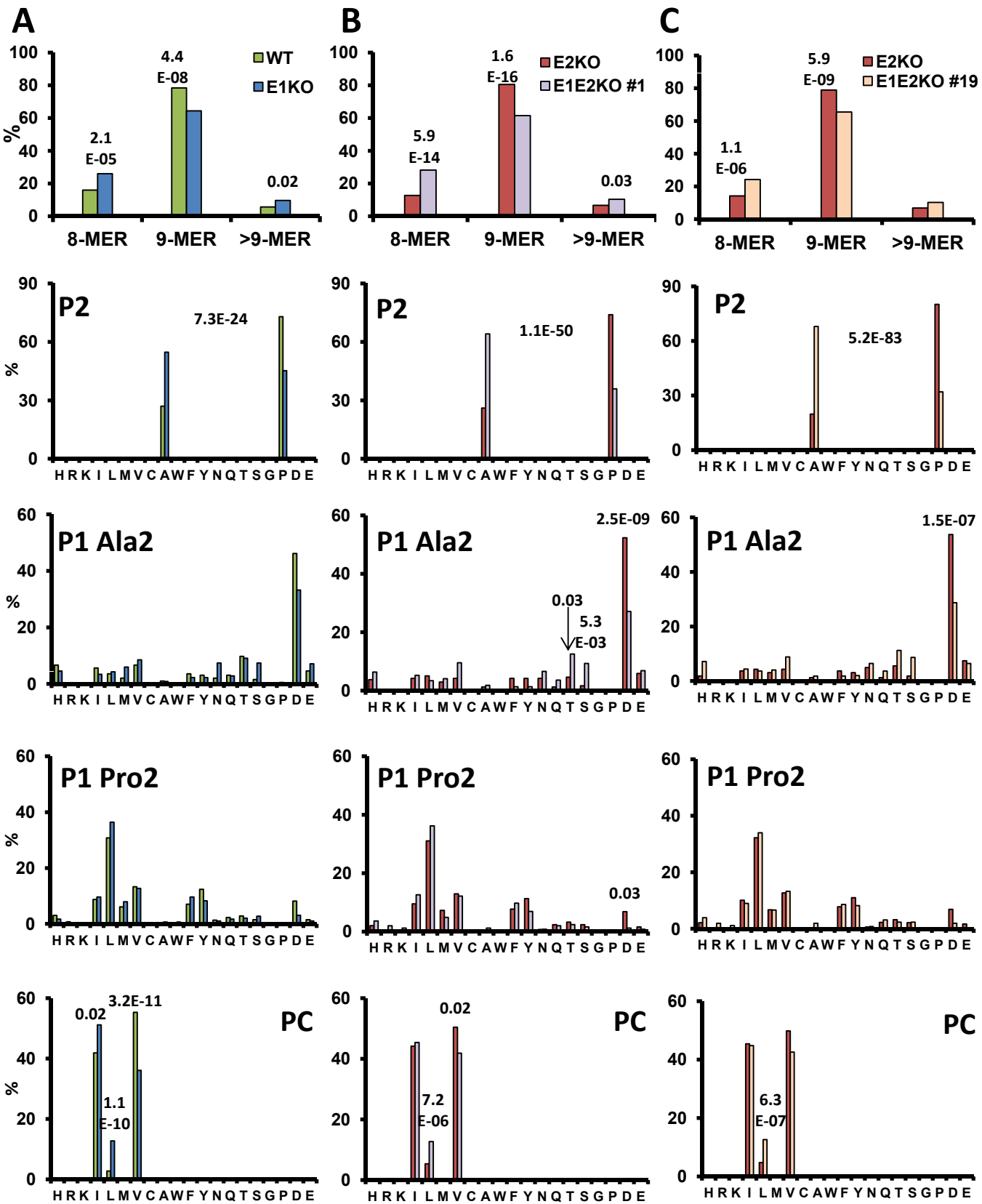
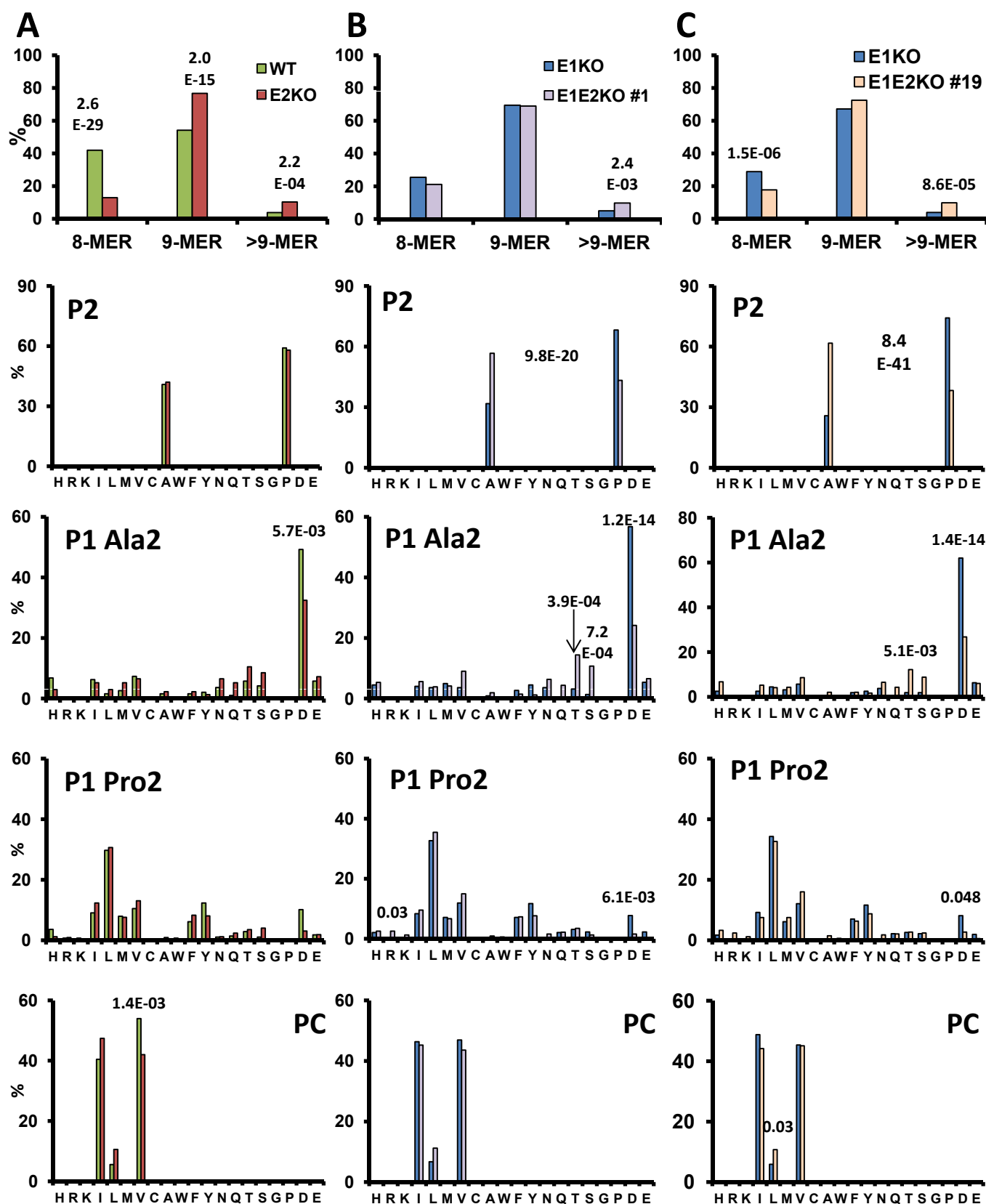


Figure 3

# ERAP2 depletion (IR>1.5)



**Figure 4**



# ERAP1+ERAP2 depletion (IR>1.5)

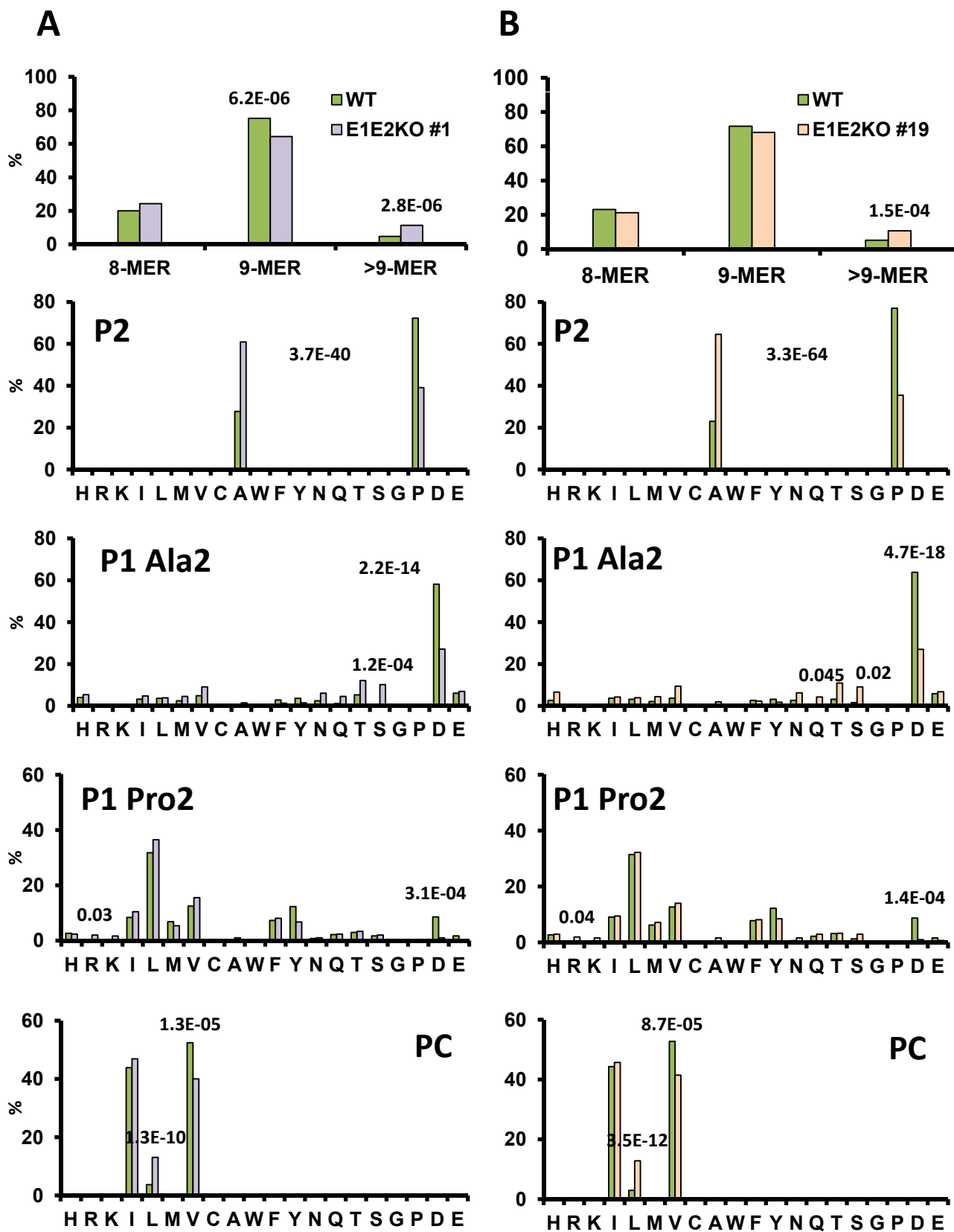


**Figure 5**

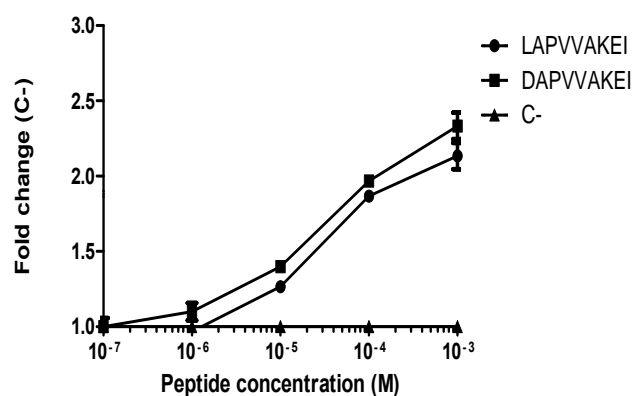
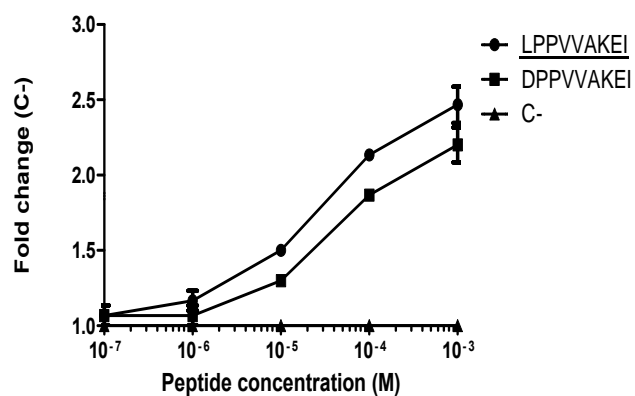
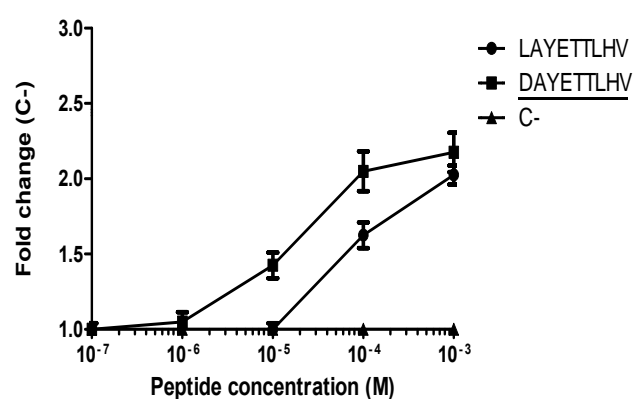
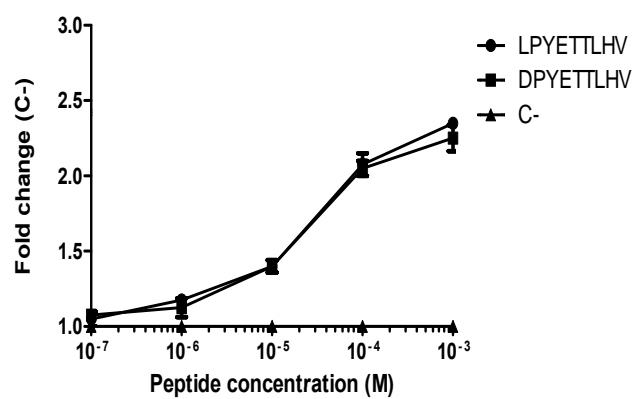


**Figure 6**

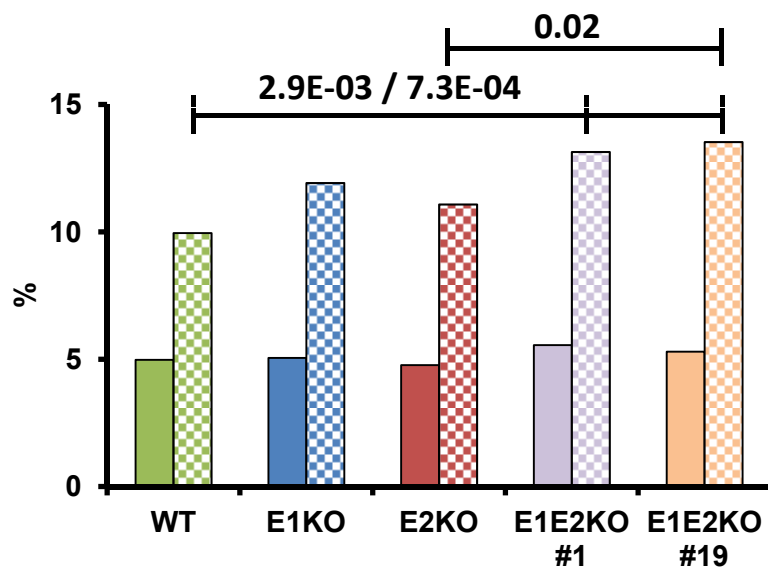


**Figure 7**